

EXPERIMENTAL METHODS OF FLOWSHEET DEVELOPMENT FOR HARD DRIVE  
RECYCLING BY PREFERENTIAL DEGRADATION AND PHYSICAL SEPARATION

by  
Brandon Ott

A thesis submitted to the Faculty and the Board of Trustees of the Colorado School of Mines in partial fulfillment of the requirements for the degree of Master of Science Metallurgical and Materials Engineering.

Golden, Colorado

Date 6/25/2018

Signed: \_\_\_\_\_

Brandon Ott

Signed: \_\_\_\_\_

Dr. Patrick Taylor

Thesis Advisor

Golden, Colorado

Date \_\_\_\_\_

Signed: \_\_\_\_\_

Dr. Angus Rockett

Professor and Department Head

Department of Metallurgical and Materials Engineering

## ABSTRACT

Neodymium-iron-boride magnet recycling by applying mineral processing practices of liberation and separation to hard disk drives is designed, discussed, and evaluated. Magnetic material, observed to be brittle, is liberated from the hard drive constructed mostly of malleable metals by preferential degradation of the magnet material.

The process developed is shown to recover greater than ninety-five percent of the neodymium-iron-boride magnet material in the feed with a product grade of up to over 80 percent magnet material by mass.

The process is designed to co-produce stainless steel, aluminum, nickel alloy, carbon steel, and printed circuit board concentrates as contributors to the recycle value of hard drives. The value of materials enclosed in hard drives is explored and discussed. Economic evaluation of this process, including estimation of capital and operating expenditures coupled with revenue based on demonstrated recovery of valuable materials, shows a positive net present value at various depreciation rates up to thirty percent.

## TABLE OF CONTENTS

ABSTRACT.....	iii
LIST OF FIGURES.....	vi
LIST OF TABLES.....	ix
ACKNOWLEDGEMENTS.....	xi
CHAPTER 1 INTRODUCTION.....	1
CHAPTER 2 LITERATURE REVIEW.....	3
2.1 Applications of Rare Earth Elements and Recycling Potential.....	3
2.2 Criticality of Neodymium.....	8
2.3 Hard Disk Drives as a Resource.....	10
2.4 Published Processes and Conclusion.....	15
CHAPTER 3 EXPERIMENTAL EQUIPMENT & PROCEDURES.....	16
3.1 Comminution Equipment.....	16
3.2 Separations Equipment.....	23
3.3 Analytical procedures and Tools.....	36
3.4 Determination of Head Grade.....	45
CHAPTER 4 RESULTS AND DISCUSSION.....	48
4.1 Analysis of Head Grade.....	48
4.2 Behavior of Shredder Output.....	48
4.3 Preferential Degradation Theory and Discussion.....	51
4.4 Initial Preferential Degradation Flowsheet.....	53
4.5 Preconcentration by Taking Advantage of Magnetic Behavior.....	58
4.6 Discussion of Co-Products contributing to viability of Process.....	60
CHAPTER 5 ECONOMIC CONSIDERATIONS.....	64
5.1 Downstream Process Considerations (product specs).....	65
5.2 Hard Drive Valuation.....	65
5.3 Estimation of Major Costs.....	71
5.4 Revenue and Process Net Present Value.....	74
5.5 Sensitivity Analysis.....	75

CHAPTER 6 CONCLUSIONS AND DIRECTION FOR FUTURE RESEARCH.....	80
6.1 Conclusions.....	80
6.2 Direction for Future Research.....	80
REFERENCES.....	81

## LIST OF FIGURES

Figure 2.1 The functional uses of the rare earth elements. Nd is used in magnets as well as minor consumption for glass and ceramics additives.....	3
Figure 2.2 Usage of Nd in its various applications. Permanent magnets represent greater than 85% of Nd consumption.....	4
Figure 2.3 Projection of in-use Nd stocks in various common applications.....	7
Figure 2.4 Projection of recycling potential for neodymium and dysprosium from common applications.....	7
Figure 2.5 The short-term criticality of materials of interest to the Critical Materials Institute. Neodymium and Dysprosium are classified as highly critical.....	8
Figure 2.6 Price History of select rare earth elements indicating the market shock of 2010-2011.....	9
Figure 2.7 Geographic distribution of hard drives across the united states.[8] .....	10
Figure 2.8 left: computer hard drive. Right: Hard drive with the back plate removed to reveal the internals. The red shaded regions indicate the assemblies containing magnet material.....	11
Figure 2.9 Disassembled hard disk drive.[9].....	12
Figure 2.10 Composition of typical hard drive by mass.....	13
Figure 2.11 The value breakdown of the above hard drive.....	13
Figure 2.12 Meta-Analysis of chemical composition of hard drive magnets compiled from several sources.....	14
Figure 2.13 Two published procedures for the generation of magnet material for testing downstream technologies.....	15
Figure 3.1 The Amos Mfg. Shredder installed in the Hill Hall Plasma Processing Lab. 1) Image of the feed chute where whole drives may be fed, 2) Shredder, 3) hang-up of magnet material on the shredder blades.....	19
Figure 3.2 Rod mill with rod charge and non-ferrous material charge.....	20
Figure 3.3 Ball mill with shredded hard drive and ball charge.....	22
Figure 3.4 image of magnet assembly before and after demagnetization.....	23
Figure 3.5 Eriez Rare Earth 15 inch drum.....	25

Figure 3.6 Low intensity magnetic drum separator.....	26
Figure 3.7 Rare Earth Roll magnetic separator.....	27
Figure 3.8 Davis Tube and Davis Tube control panel.....	28
Figure 3.9 Eddy current separator.....	29
Figure 3.10 Shaking Table. The heavy fraction comes off the left side of the table, The light fraction comes off the right side over the ridges.....	30
Figure 3.11 Air table density separation equipment.....	31
Figure 3.12 Gilson screen (left) with screens installed. Dust cover installed (right) with air draw to bag house visible at bottom of the image.....	33
Figure 3.13 Ro-tap screen stack.....	35
Figure 3.14 Results of XRF scans on standards.....	37
Figure 3.15 Pulverizer for fine grinding of XRF samples.....	39
Figure 3.16 Press used to prepare XRF samples.....	40
Figure 3.17 Fuser used for preparation of fused samples.....	41
Figure 3.18 Standardization Curve for ICP-MS results.....	42
Figure 3.19 Fire assay bead in cupel.....	45
Figure 3.20 Sorted metals from shredded hard drive.....	46
Figure 4.1 Percent passing curves for the shredder output from several shredder manufacturer.....	49
Figure 4.2 Shredder particle size analysis for several variations of shredding procedure including multi-pass shredding and the effect of demagnetization before shredding.....	50
Figure 4.3 Results of magnet hammering experiment.....	51
Figure 4.4 Concept preferential degradation flowsheet.....	53
Figure 4.5 Initial screened preferential degradation flowsheet.....	54
Figure 4.6 Magnetic circuit for upgrading of process output.....	55
Figure 4.7 Wet and dry screening analysis of preferential degradation process outputs.....	56

Figure 4.8 Conceptual preconcentration flowsheet.....	57
Figure 4.9 Preferential degradation flowsheet.....	58
Figure 4.10 Preconcentration flowsheet with results from analysis of outputs.....	59
Figure 4.11 Conceptual material destination flowsheet. The further processing of the fine fraction is by a range of processes, for example sulfation roasting.....	61
Figure 5.1 Value of neodymium grade for selective sulfation roasting. The minimum cutoff grade for profitability is about 10% neodymium by mass.....	64
Figure 5.2 Charts showing the material composition, inherent value, and recovered value.....	67
Figure 5.3 Hard drives from a range of years. Clockwise from top left: 2003, 2008, 2011, and 2010. All Hitachi deskstar model hard drives.....	68
Figure 5.4 Sensitivity of net present value to various costs.....	76
Figure 5.5 Sensitivity of net present value to material recoveries.....	77
Figure 5.6 Sensitivity of net present value to project life.....	78
Figure 5.7 Sensitivity of NPV to service charge.....	79

## LIST OF TABLES

Table 2.1 Typical Lifespan of consumer products containing rare earth magnets.....	5
Table 2.2 Estimated Global in use stocks of rare earth elements in 2007.....	6
Table 2.3 Average composition of hard drive magnets (wt.).....	15
Table 3.1 Stanardization sample compositions with known amounts of added oxide. MGBM samples are based on process output and XRF samples are based on a ground pure magnet. 4 samples are spiked with neodymium oxide and 2 samples with silica.....	36
Table 4.1 Table of several disassembled Hitachi Deskstar HDDs used to compute the head grade of the process.....	48
Table 4.2 Magnet particles found in various screen fractions by hand sortation.....	51
Table 4.3 Table of upgrade studies on ball mill output.....	55
Table 4.4 Demonstrated material recoveries of co-products.....	63
Table 5.1 The values of the materials found in hard disk drives. These are reduced in some cases to represent uncertainty and impurities.....	65
Table 5.2 Printed circuit board value based on fire assay results. This represents the total entrained commodity value and must be reduced to represent the challenges of recovery from the circuit board. The value displayed in figure 5.1 is based on this data.....	65
Table 5.3 The entrained circuit board value from previous research [16].....	66
Table 5.4 Table of Recovered Value from shredded hard drive process.....	66
Table 5.5 composition data of magnets from several manufacturers.....	68
Table 5.6 Deconstruction results of the 4 hard drives shown above. The matrix on the left shows the mass breakdown of each drive. The matrix on the right shows the value of those components and the total value of the drive.....	69
Table 5.7 Circuit board values from Hitachi Desk-Star hard drives with various dates of manufacture.....	69
Table 5.8 Capital expenditure (CAPEX) table. Major equipment costs are based on manufacturer budgetary prices. Cost factor calculations are used to determine various additional capital costs.....	71
Table 5.9 Operating expenditures. The HDD delivery, labor, and electric power	

contribute most significantly to the cost.....	72
Table 5.10 Model including both operating and capital expenditures in the appropriate time periods from the estimates discussed above.....	73
Table 5.11 Cashflow model.....	74

## DEDICATION

This research was completed with support from the Critical Materials Institute and I would like to extend my gratitude to them for that support.

I would like to sincerely thank my advisor Dr. Patrick Taylor as well as my committee members Dr. Corby Anderson and Professor Erik Spiller for their ongoing advice and the opportunity to conduct this research.

I would also like to thank my fellow Kroll Institute for Extractive Metallurgy students for all the hours they have loaned to me and the insight they have provided.

Many thanks are deserved by my girlfriend Marley Smith for her constant love and support during this project.

My Friends, Ryan, Zach, and Tyler. I am thankful for the healthy distractions that you have provided.

Finally, I would like to thank God for giving me the knowledge, the ability, and the opportunity to complete this research.

Without these people this project would have been impossible to complete.

## CHAPTER 1: INTRODUCTION

Neodymium Iron Boride magnets are used for their relatively high magnetic field potentials relative to other magnet materials. They are primarily composed of the phase  $\text{Nd}_2\text{Fe}_{14}\text{B}$  but often contain amounts of Praseodymium and Dysprosium. Praseodymium is a low-cost replacement for Nd in the magnetic phase while Dysprosium improves the thermal stability of the magnets for certain applications. These materials are considered critical due to both supply and demand concerns. Supply is dominated by The People's Republic of China which has shown a willingness to leverage rare earth metals prices in foreign negotiations. The lack of domestic supply contributes to a volatile rare earth market. The demand is expected to increase due mainly to the growth of the electric car market. The domestic capacity to fulfill the current demand or the future demand growth is extremely limited. It is hoped that recycled materials could contribute significantly toward supplying this domestic demand and growth. One potential domestic supply is computer hard disk drives. These drives are disposed of by shredding upon end of life for data security. It is estimated that about 115million HDDs are decommissioned annually in America and up to 325million HDDs worldwide per year. Of these about 50% are refurbished and resold and 25% are either shredded or smelted. The remainder are not recycled. It is estimated that 10-15 million hard drives are shredded annually in the United States. The recovery of neodymium-iron-boride magnet material from shredded hard drives is the goal of this research. The Critical Materials Institute's stated objective for this project is the development of a deployable, economically sound method for the recycling of rare earth elements, particularly neodymium, from "post-consumer magnet bearing devices." The specific focus of this process development is for the recycling of hard drives particularly by shredding.

Rare earth magnet material is to be recovered along with aluminum, stainless steel, nickel, carbon steel, and possibly printed circuit boards (PCB). The majority of the entrained value is found in the aluminum, nickel, stainless steel, PCB, and magnet fractions. The processes developed by this research are evaluated based on estimates of the value of process output streams and estimates of necessary equipment and operating costs to build and operate such a plant.

The Critical Materials Institute has additional projects focused on the separation of neodymium from iron in magnet material. The communication with these potential downstream

process development projects allowed evaluation of the process output to determine its suitability for an integrated extraction process. The possibility of direct reuse of the produced magnet concentrate was also considered and discussed.

## CHAPTER 2: LITERATURE REVIEW

### 2.1: Applications of Rare Earth Elements and Recycling Potential

Rare earth elements are a group of 17 elements that include scandium, Yttrium, Lanthanum, and the lanthanoids; Cerium, Praseodymium, Neodymium, Promethium, Samarium, Europium, Gadolinium, Terbium, Dysprosium, Holmium, Erbium, Thulium, Ytterbium, & Lutetium. Of these Yttrium, Neodymium, Europium, Terbium and Dysprosium are considered critical materials.

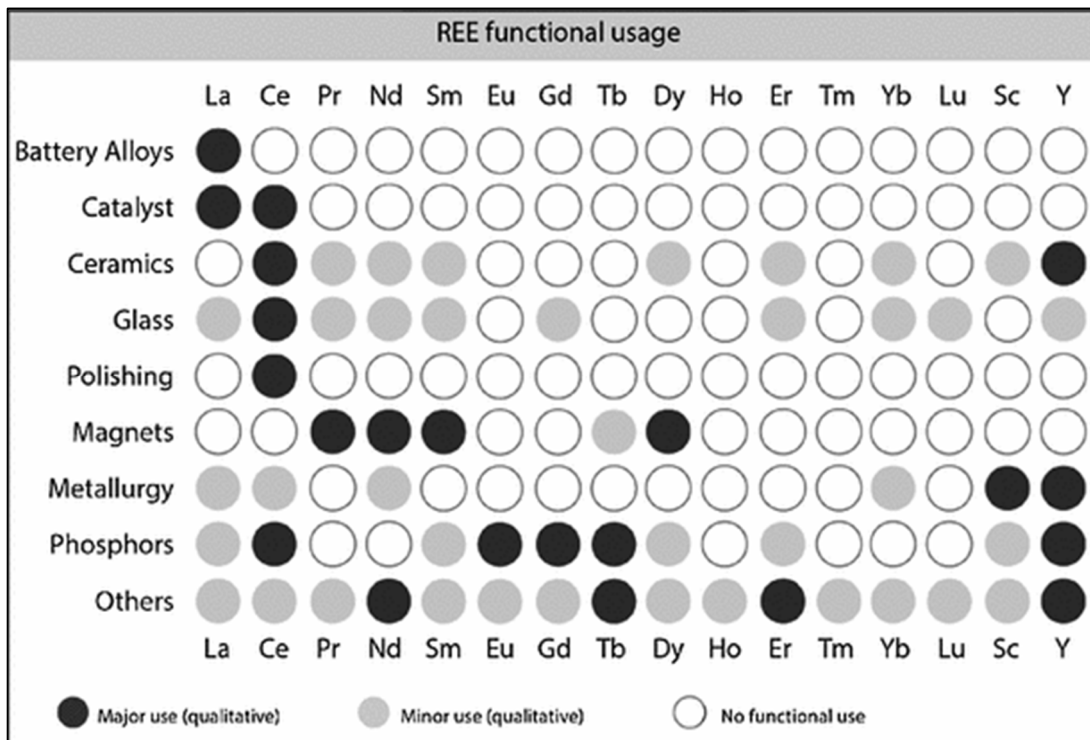


Figure 2.1: The functional uses of the rare earth elements. Nd is used in magnets as well as minor consumption for glass and ceramics additives.

Neodymium has particular market value particularly due to its use in intermetallic magnet alloys commonly used in consumer electronics and electric motors. These magnets are commonly found in electric vehicles, wind turbines, and hard disk drives as well as consumer appliances and other household electronics. This implementation of neodymium rare earth magnets is mostly due to their strong magnetic field potential and high specific magnetism (high magnetic field to mass ratio). [2]

Neodymium is mostly found in ores among a mixture of rare earth elements (REEs). Most neodymium production is as part of generic mixed REE production from these deposits. The most common Neodymium production is from Bastnaesite beneficiation through an acid roasting procedure that produces a RE sulfate. Most neodymium production statistics originate from the China Rare Earth Information Center. Total neodymium production in 2007 was in excess of 21,000 tons. Neodymium magnet production was estimated at 70,000 tons. This data indicates that 85% of neodymium production goes into magnet materials. Other applications for neodymium include glass dye additives, catalytic converters, and ceramic additives. There is a large energy cost to mining rare earth elements and so reuse or recycling is hoped to reduce the carbon footprint of production as well as providing a stabilizing market source from diversification of supply. It is noted that there is more installed production capacity than the current market equilibrium. There is very little potential for recycling from any of the applications other than permanent magnets due to their market share of neodymium consumption. [3]

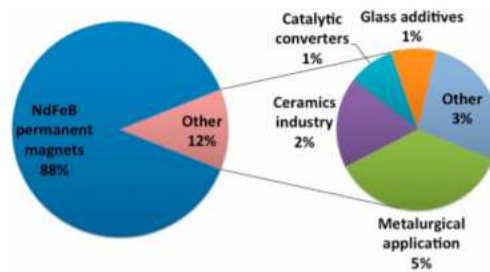


Figure 2.2: Usage of Nd in its various applications. Permanent magnets represent greater than 85% of Nd consumption.

Du and Graedel identify the product lifetime for common rare earth magnet applications of particular interest for this project is the 10-year lifetime referenced for computer technologies. It is expected from this that the process input would be composed of approximately decade old hard drives. It is noted in the introduction above that more than 50% of decommissioned drives are refurbished and see additional service. It would be expected that this would lengthen the gap

Table 2.1: Typical Lifespan of consumer products containing rare earth magnets.

<i>Products</i>	<i>Life span (yr)</i>	<i>Reference</i>
Computers	10	Matthews and colleagues (1997), Babbit and colleagues (2009)
Audio systems	10	Modified from Oguchi and colleagues (2008)
Wind turbines	20	Grauers (1996), Lipkin (2009)
Automobiles	14	Staudinger and Keoleian (2001)
Household appliances	15	Reck and colleagues (2008)
MRI	10	Adjusted from <a href="http://www.ehow.com/about_4731161_much-do-mri-machines-cost.html">http://www.ehow.com/about_4731161_much-do-mri-machines-cost.html</a>

between production and recycling and distort the normal distribution to longer gaps between production and recycling (Table 2.1 on page 5).

Du and Graedel in “Global rare earth in-use stocks in NdFeB permanent magnets” determined the in-use stock of magnets in 2007. This is calculated using global production statistics and several sources of end use information. The stocks of individual rare earth elements are about four times the annual extraction rate. This suggests that there is sufficient rare earth material in circulation that recycling of these materials may have a significant impact on the REE supply in the future. It is noted that the in-use stocks of all metals are growing, however it is expected that the stocks of rare earth elements will grow faster than other sectors. This is due to the expected growth of stocks mainly in electric motors and wind turbines that are expected to increase drastically as technology and politics drive their adoption. By combining in use stocks and expected product lifetimes an estimate of the discard rate can be predicted into the future (Table 2.2 on page 6).

The stocks are compared to demand and this comparison is projected into the future by Rademaker et al. This is shown in Figure 2.3. It is expected that the growth of stocks will outgrow the demand growth for neodymium oxide. Most of this growth is expected in the automotive and wind energy sectors. [4]

Table 2.2: Estimated Global in use stocks of rare earth elements in 2007.

<i>Stocks (Gg)</i>	<i>Nd</i>	<i>Pr</i>	<i>Dy</i>	<i>Tb</i>	<b>Total</b>
Computers	21.2	5.3	5.3	1.1	<b>32.8</b>
Audio systems	15.1	3.8	3.8	0.8	<b>23.4</b>
Wind turbines	10.1	2.5	2.5	0.5	<b>15.7</b>
Automobiles	9.8	2.5	2.5	0.5	<b>15.2</b>
Household appliances	3.3	0.8	0.8	0.2	<b>5.1</b>
MRI	3.0	0.8	0.8	0.2	<b>4.7</b>
<b>Total</b>	<b>62.6</b>	<b>15.7</b>	<b>15.7</b>	<b>3.1</b>	<b>97.0</b>

The potential recycling supply of neodymium and dysprosium is shown in Figure 2.4 on page 7. The current potential is notably in HDD recycling with potential for recycling automotive REE resources as well as wind turbine generators not contributing significantly to the recycling potential until the mid-2020's. [5]

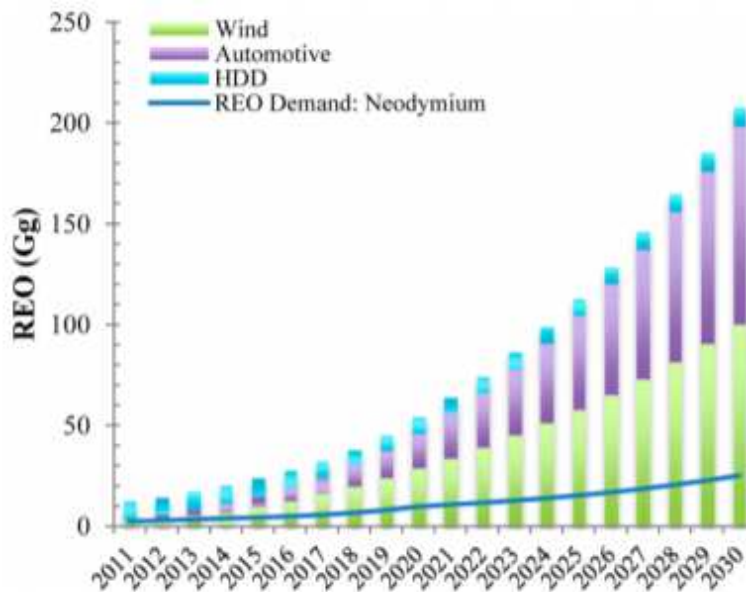


Figure 2.3: Projection of in-use Nd stocks in various common applications.

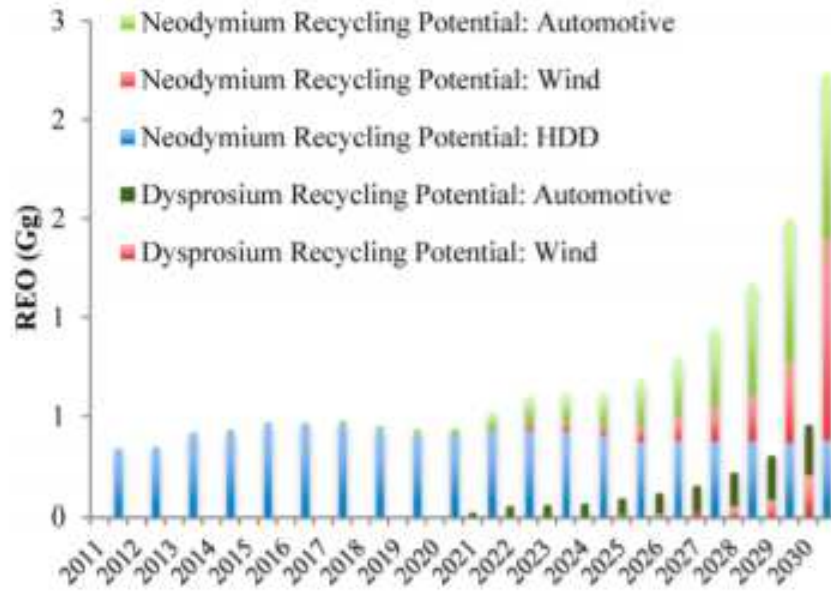


Figure 2.4: Projection of recycling potential for neodymium and dysprosium from common applications.

## 2.2: Criticality of Neodymium

Neodymium is considered a critical material in the department of energy’s critical materials strategy initially identified as such in 2011. Dysprosium, also found in RE magnets, is considered critical as well. Criticality is based on some combination of supply risk and substitutability in common applications. It would be said that a material has a high level of criticality if there are high risks to supply and high essentiality for the material in its common applications. Criticality does not necessarily suggest that there is an equilibrium supply shortage but rather that there is significant risk to supply and dire consequences of that risk. Nd is classified as a highly critical material primarily because of supply risk (Figure 2.5 on page 8). [6]

The consequences of neodymium supply risks can be observed in the price history of neodymium and dysprosium and a market shock in 2010 (Figure 2.6 on page 9). The neodymium price in 2011 was 10 times the previous price and dysprosium peaked at 25 times its previous price.

This market shock was due to a geo-political supply concern from the market’s preeminent supplier. The exact cause of the shock is unknown however the results are obvious. During this crisis the Japanese government announced a plan to treat scrap sources of REEs as a resource. Growth of global rare earth production is somewhat limited due to several investment

and political concerns. The rare earth mining sector sees limited investment due to large uncertainty even relative to other mining projects. The uncertainty in rare earth price several years from the investment date after mine design, construction and commissioning creates problems for investment. It is unknown if the mine process will be profitable based on future rare earth prices.

There is always investor hesitation in long term projects where payback period is subject to uncertainty and unpredictable events over long periods of time. There is also the fact that the Chinese government is actively trying to reduce unlicensed rare earth mining operations, these operations are a significant contributor to global production and so their sequestration may reduce the total global output even as additional mines are built. [6]

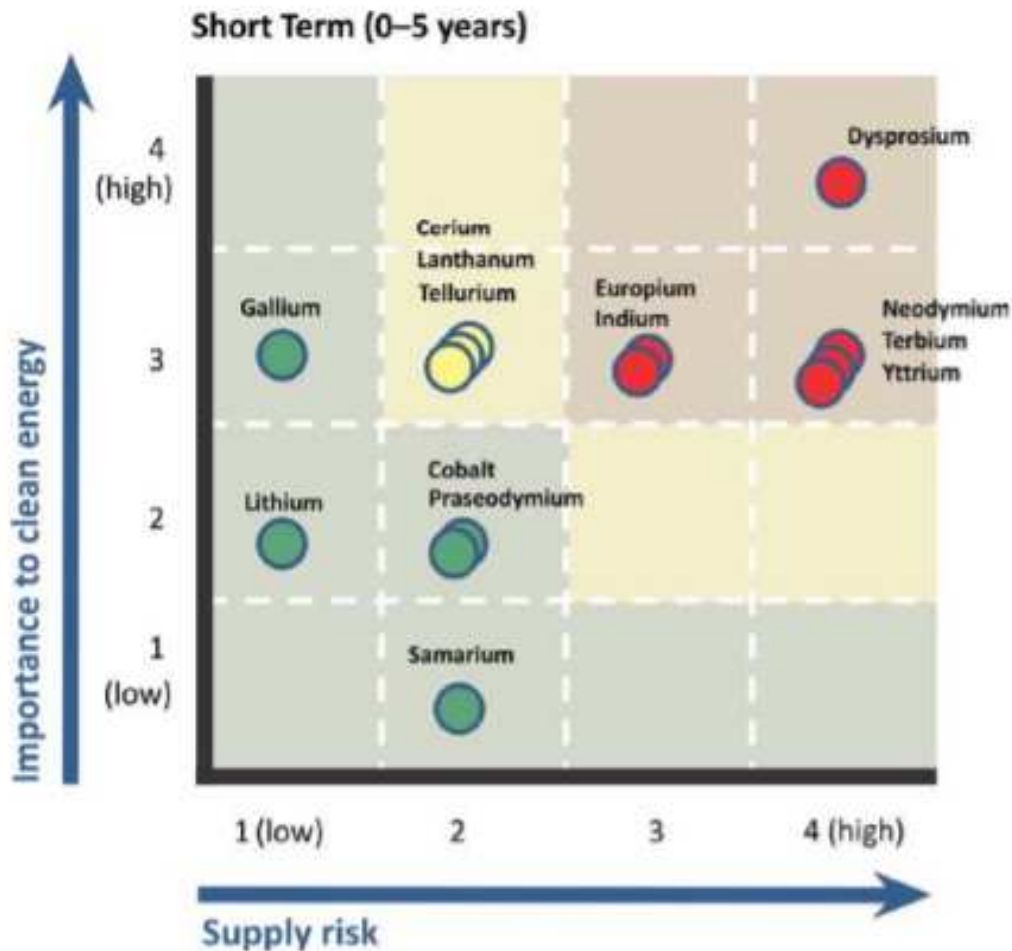


Figure 2.5: The short-term criticality of materials of interest to the Critical Materials Institute. Neodymium and Dysprosium are classified as highly critical.

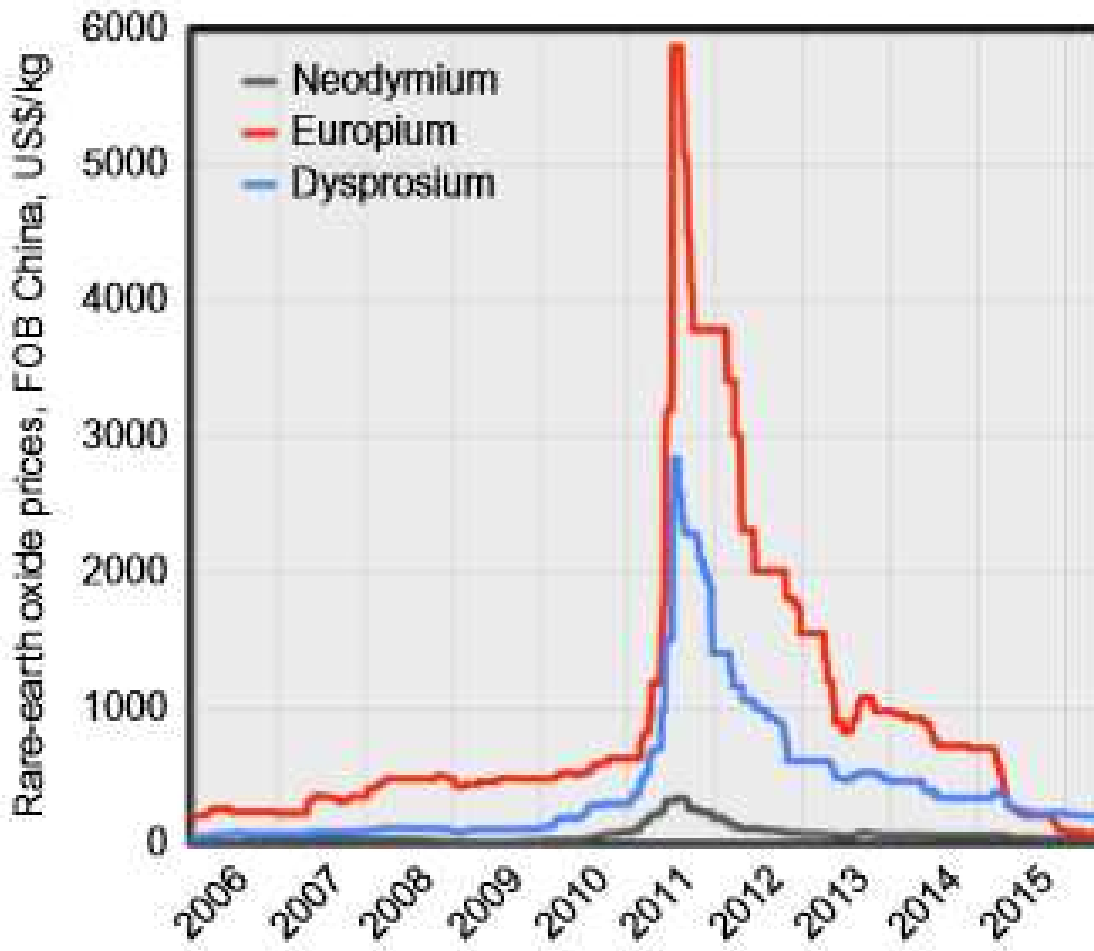


Figure 2.6: Price History of select rare earth elements indicating the market shock of 2010-2011

### 2.3: Hard Disk Drives as a Resource

Dahmus and Gutowski considered the range of materials that are successfully recycled. They show that simple objects, such as glass containers are more economical for recycling. A high level of mechanical complexity or objects composed of highly mixed materials is detrimental to recycling processes. Collection costs are often a concern for recycling projects. They often times represent a large operating expenditure that can significantly reduce commercial viability. Collection and logistics must be accounted for in discussions of project viability. Recycling is currently a small contributor to global rare earth supply. This is in part a result of the extraction cost due to the general complexity of rare earth containing devices. [7] The cost of extraction from end of life consumer waste can be even greater than the cost of extraction from ore. Collection presents significant challenges and so large-scale users represent a better source than products dispersed among personal users, i.e. individual households. [7]

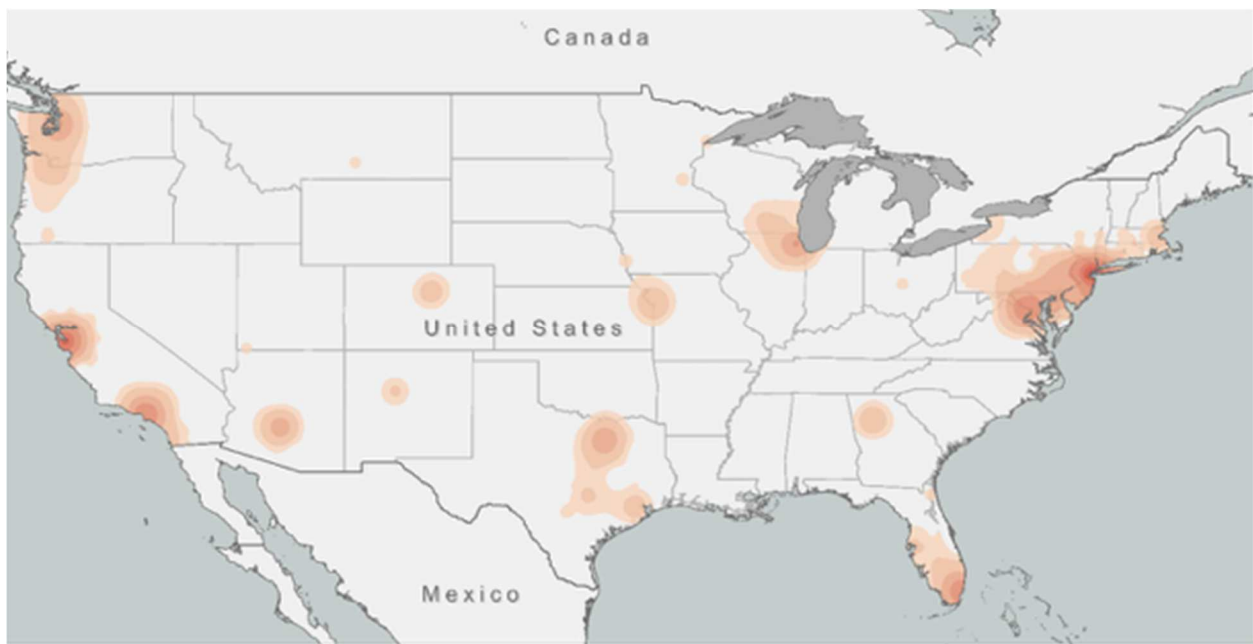


Figure 2.7: Geographic distribution of hard drives across the united states. [8]

In hard drives, magnets are concentrated in the spindle motor assembly (red ring) as a bonded magnet for driving the disk rotation as well as a separate magnet assembly for the voice coil (lower left corner). The surrounding materials are mostly metals, with minor amounts of circuit boards and plastics. The platter that must be destroyed for data security is the aluminum

disk centered around the previously mentioned spindle motor magnet visible in Figure 2.8. Hard drives often contain several of these platters in a stack. [9]



Figure 2.8: left: computer hard drive. Right: Hard drive with the back plate removed to reveal the internals. The red shaded regions indicate the assemblies containing magnet material.

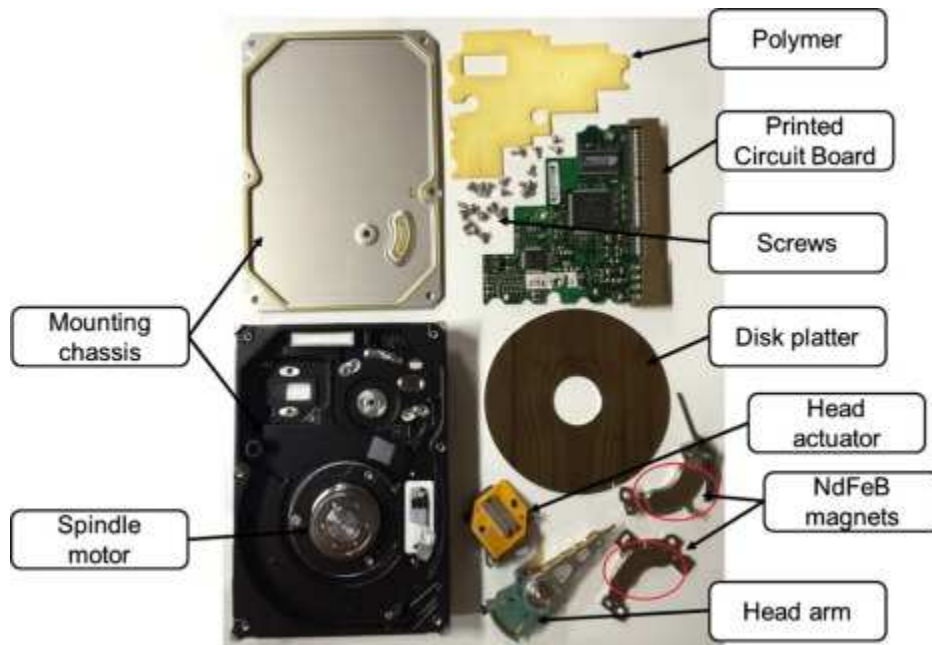


Figure 2.9: Disassembled hard disk drive.

Literature includes evaluation of hard drive composition analysis; the rare earth magnet material is concentrated in 2 places within the hard drive assembly. This fits into the definition of a complex, hard to recycle structure according to Dahmus and Gutowski as discussed above. It

should be noted that hard drives have a shorter service life and are relatively less complex than other high-volume rare-earth stocks including automobiles and wind turbines. In hard drives there is also a notably high level of diversity in material leading to additional challenges in recycling.

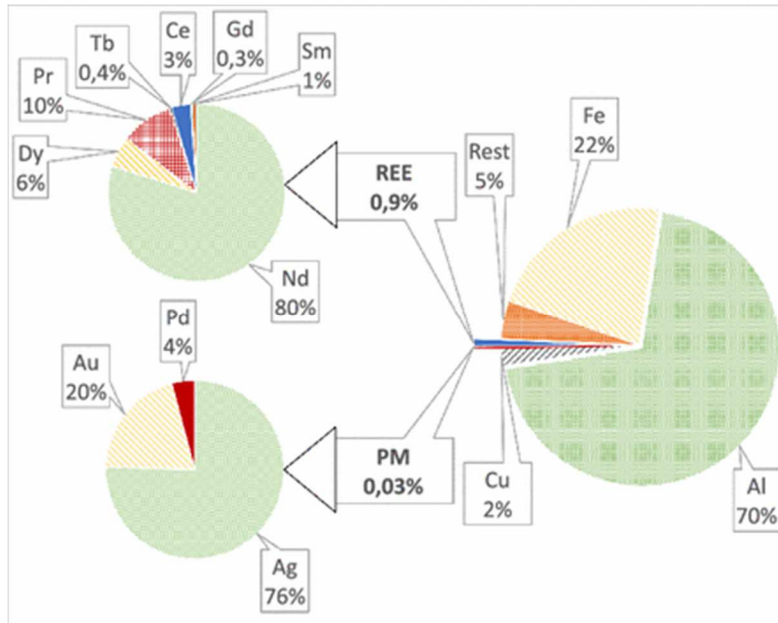


Figure 2.10: Composition of typical hard drive by mass.

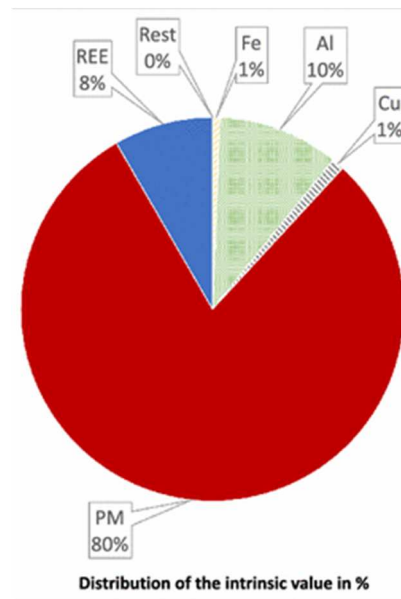


Figure 2.11: The value breakdown of the hard drive.

Upon complete deconstruction the various components can be identified. The voice coil magnets can be of various sizes, some higher capacity hard drives have multiple platters. The magnets are held onto the magnet bracket by both magnetic force and by epoxy.

The hard drive case and disk platter are generally aluminum. The front plate is either carbon-steel or stainless steel depending on manufacturer and date. The magnet bracket is a nickel alloy. The hard drive is by mass mostly aluminum with significant components composed of plain carbon steel or stainless steel as is the server bracket. The magnet and printed circuit boards are analyzed further. The magnet material consists mostly of Nd but also includes some praseodymium and dysprosium. The circuit boards are analyzed to include significant gold and silver. Most of the circuit board is copper and plastic. The value of these components is mostly associated with the precious metals fraction. The rare earths are not the primary contributor to hard drive intrinsic value but due to criticality their recycle is of particular interest.

The analysis of magnet material from several hard drives shows the expected composition especially in terms of rare earth content. Both the spindle motor magnet and the voice coil magnet are analyzed. The nickel that is present in the voice coil magnet is from the coating that prevents oxidation of the  $Nd_2Fe_{14}B$  material. There is significant variation in the magnet composition with Nd content ranging from 17 to 27% by mass. This variation is mostly different between manufacturers and dates of manufacture rather than in individual hard drive models. [9]

Another source listed the following for average composition of magnets in weight percent (Figure 2.12 on page 14). This is compiled from several authors. [10]

Table 2.3: Average composition of hard drive magnets (wt.%)

Element	Nd	Pr	Dy	Fe	B	Co
Average	25.3	3.83	2.66	64.56	0.97	2.42

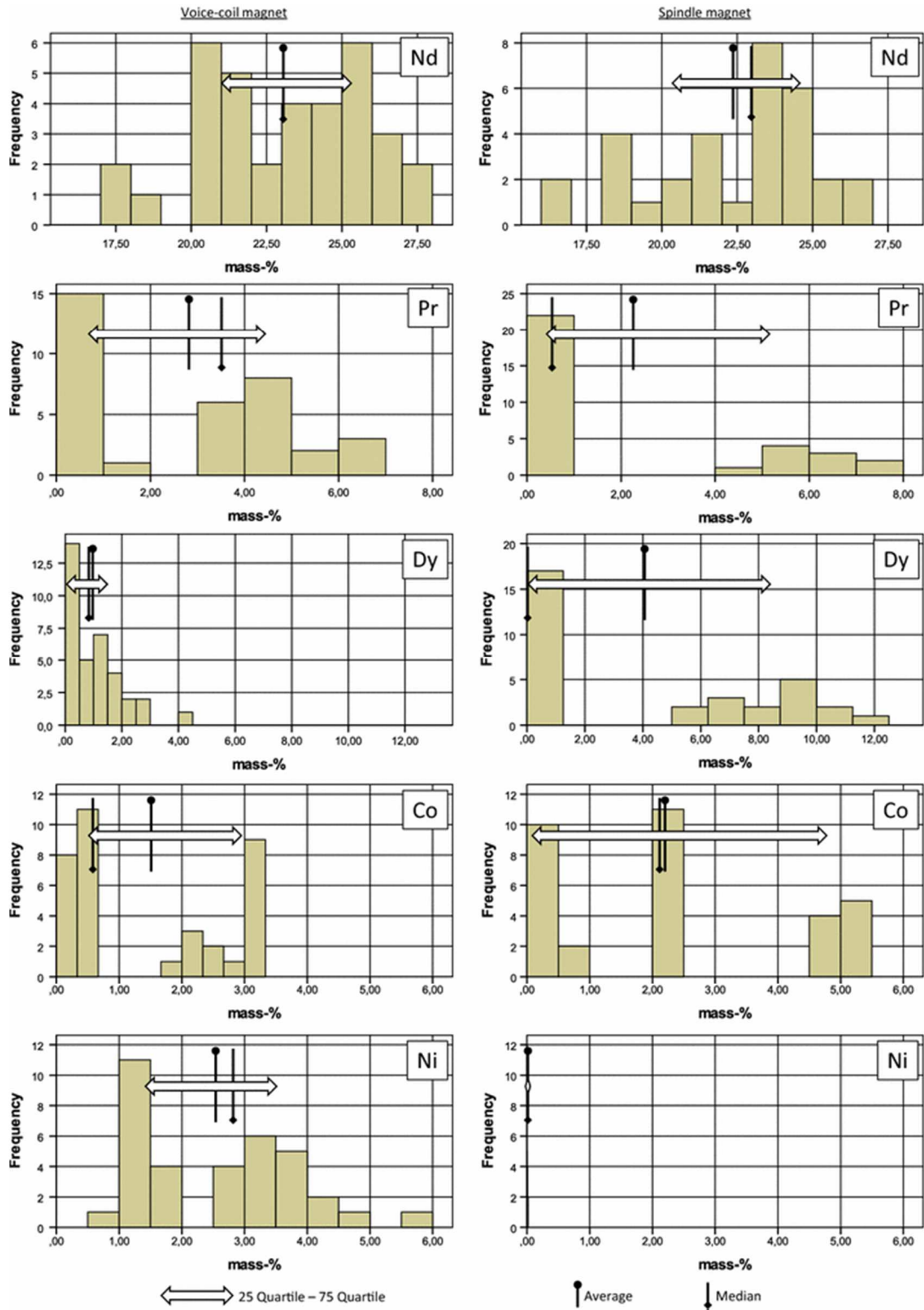


Figure 2.12: Meta-Analysis of chemical composition of hard drive magnets compiled from several sources.

## 2.4: Published Processes and Conclusion

During the course of this research additional papers became available that represented results similar to the initial scoping studies. München et al. describe a process of manual dismantling and thermal demagnetization followed by grinding the coated magnet material for Nd recovery.

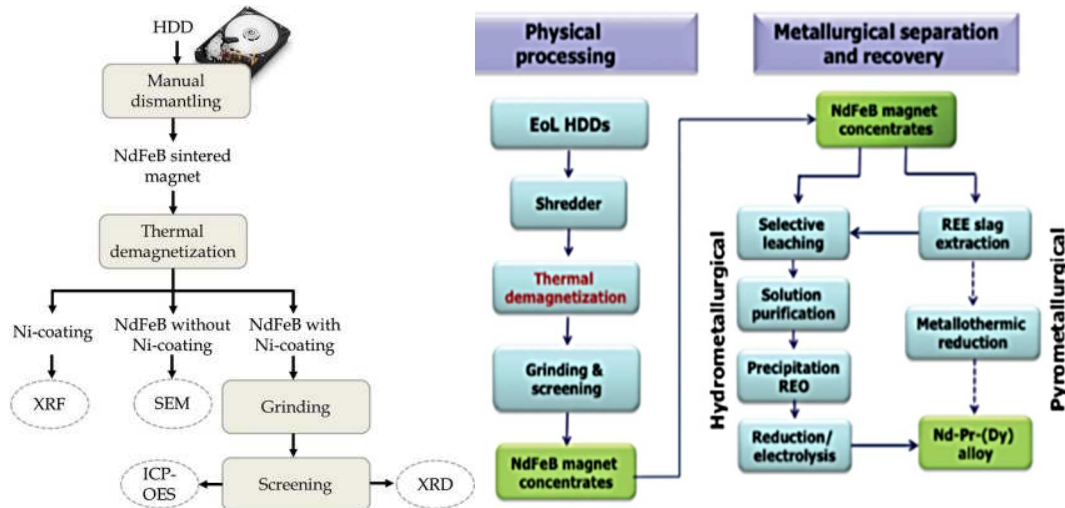


Figure 2.13: Two published procedures for the generation of magnet material for testing downstream technologies.

Additionally, Abrahami et al. presented a process by which end of life hard drives are shredded, demagnetized, and ground to produce a magnet material concentrate. Their primary concern was the development of a hydrometallurgical process for separating NdFeB into its constituent components. The hard drive shredding process produced a feed for the hydrometallurgical process. Neither of these projects attempted to recover value from the other materials in the hard drives. These 2 papers indicate that the initial research can be duplicated and that the fundamentals of this project are sound. [11] [12]

Hitachi has published a recycling process that is currently being implemented commercially for separation of rare earth magnets from used products. This is part of their resource recycling initiatives. Their recovery of rare earth magnets is primarily from HDDs and air conditioner compressor motors. Magnets are liberated from HDDs by disassembly. Various materials are recovered by gravity concentration, magnetic separators, and a vibrating filter. Hand sorting is used in various steps in the process. [13]

Bandara et al. determined the neodymium concentration in mixed shredder scrap output. They showed a drum magnetic separator concentrating neodymium to the ferrous fraction but did not develop further process steps. [14]

Walton et al. developed a process by which neodymium magnets could be extracted from hard drive bodies by decrepitation via hydrogen exposure of the magnets. This process showed a recycled product made by recycling of the magnet compound with some loss of magnetic properties. [15]

There are various additional researchers who have developed technologies to separate neodymium (and other rare earths) from the iron in the magnet compound.

Based upon the literature survey it can be seen that there are significant sources of neodymium available for recovery from computer hard drives that may help address the criticality of the rare earth element. The value of a process that recovers neodymium should also recover other materials as the rare earths are a small contributor to the intrinsic hard drive value. There is potential for a recycle process to exploit the current stock of neodymium and other rare earth elements in end of life hard drives to provide a significant domestic supply. The goal of this process development is to minimize the effect of supply shocks by diversification of supply for neodymium. This in-turn would reduce the criticality of neodymium.

## CHAPTER 3: EXPERIMENTAL EQUIPMENT & PROCEDURES

Experiments were carried out in the Laboratories of the Kroll Institute for Extractive Metallurgy at the Colorado School of Mines. On campus there are several pieces of equipment for both comminution and separations unit operations that allowed the testing necessary for this thesis. Process equipment, particularly those that will retain magnetic material are cleaned before and after processing.

### **3.1: Process Equipment**

#### **3.1.1 Crushing**

The primary crushing apparatus used for hard drive comminution is a shredder. Several shredders are used for the initial experimentation and flowsheet design but subsequent research is accomplished by shredding with an Amos mfg. dual cam shredder installed at the Colorado School of Mines. This shredder is capable of shredding hard drives one or two at a time. Slow speed shear shredders of the sort installed at CSM are capable of shredding a wide range of materials including; tires, metals, cars, wood products, plastics, and electronic waste. The mechanism of comminution is mostly shearing which is capable of degrading both brittle and malleable materials making this sort of comminution particularly useful for crushing of mixed materials including metals and other materials. Some processes considered included demagnetization prior to shredding which minimizes accumulation of magnetic material on the shredder cams. If the feed material is not demagnetized the unit is thoroughly cleaned after use. It was found that feed jams were minimized by running oil through the cams for a short time (2-3 mins) before starting large shredding volumes. Jams occurred when the shredder was overfed especially when multiple hard drives were stuck together by melted plastic. Larger hard drives were fed slower than less massive drives.

Operation Procedure:

1. Shredder is turned on starting with the breaker box, then the internal breaker, and finally the initialization of the shredder control box by key.
2. Before shredding 3in1 oil is added to the cams directly and the shredder is started and run for 2-3mins.
3. A receptacle is installed below the shredder on a jack stand that is raised to seal onto the shredder discharge prior to shredding.

4. It is recommended that the bag house be turned on to extract fines produced by the shredder, this is done with the green “start” button on the bag house control panel.
5. The shredder is shut off with the red “stop” button before being opened and fed hard drives. It is recommended that hard drives be fed 1-2 at a time and that they not be stuck together to minimize jams.
6. In the case of a jam the shredder will automatically reverse direction to clear the jam and continue shredding
7. If the jam is not cleared there are several steps to take to clear a shredder jam.
  - a. The reverse direction function can be operated manually and longer durations of reverse operation might clear small jams
  - b. If the shredder is to be opened lockout procedure must be followed to insure safety

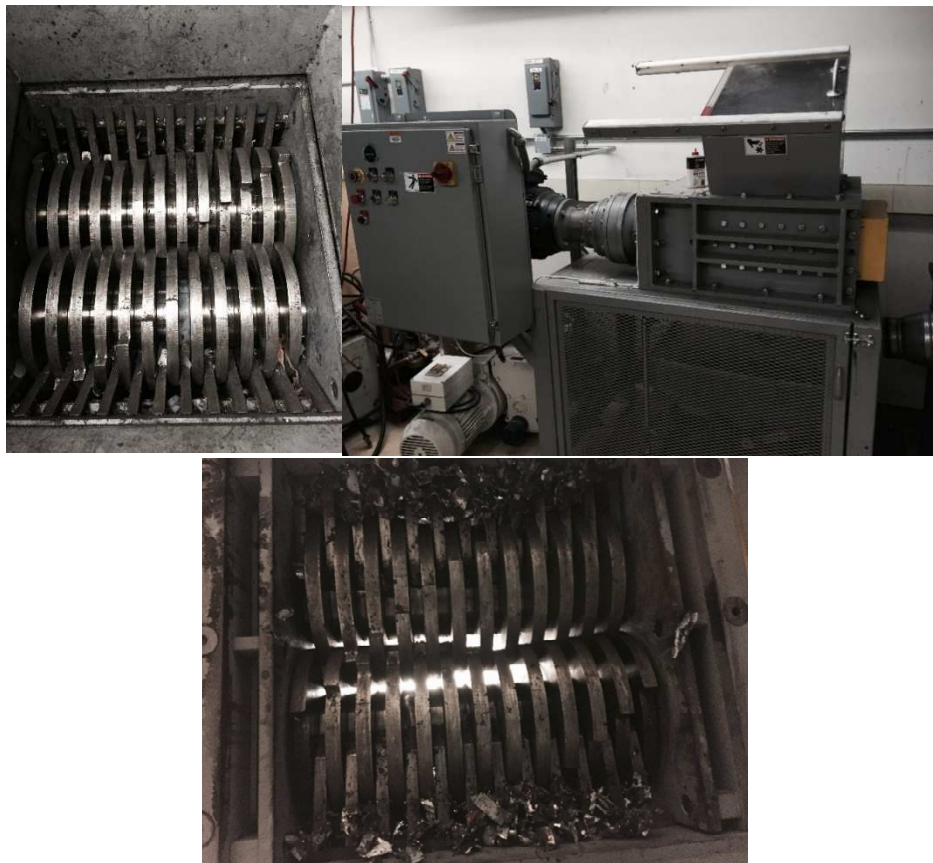


Figure 3.1: The Amos Mfg. Shredder installed in the Hill Hall Plasma Processing Lab.  
1) Image of the feed chute where whole drives may be fed, 2) Shredder, 3) hang-up of magnet material on the shredder blades.

- c. The shredder jam can be cleared by pushing material through the cams using a punch or by pulling material from between the cams using pliers
8. If the fence below the shredder or the window covering the feed chute is opened during operation the shredder cams will stop rotating, the window and grate must be closed before shredding

### **3.1.2 Grinding:**

There are 2 grinding mills used in this research for different testing scales. Both of these mills are of a steel construction and so magnet material is demagnetized prior to grinding to enable discharge of magnet material. The laboratory scale tests with single digit hard drive quantities are completed in a laboratory jar-rod mill.

The rod mill is a 7x11 inch mill with a rod charge of about 4kg. Grinding time varied between 1 and 2 hours. The rod mill is cleaned and rinsed prior to use and dried with compressed air prior to charging. After grinding the material is brushed out of the mill into a receptacle container.

Rod Mill Procedure:

1. Rod mill container as well as grinding media is cleaned thoroughly before use
2. Grinding media is added to the mill jar
3. Material is added to the rod mill jar
4. Lid is put on the top of the mill jar and clamped using the lid clamp.
5. The lid must be clamped tightly to ensure that the lid does not come off inside the grinding chassis
6. Jar is placed into the grinding chassis which is subsequently plugged in to start motion
7. The material is carefully removed from the grinding jar
  - a. Rods are removed first and brushed into a receptacle
  - b. Material remaining in mill is poured into a receptacle
  - c. Jar walls are brushed clean into a receptacle



Figure 3.2: Rod mill with rod charge and non-ferrous material charge.

Larger samples are processed by a custom built one-meter ball mill installed in the Earth Mechanics Institute at Colorado School of Mines. This mill is capable of milling on the scale of 100kg of material with 2.5” steel balls. The larger mill is capable of higher energy impacts than the laboratory scale mill which is more effective for preferential degradation. The higher energy impacts tend to improve recovery of brittle material to the fine fraction. Grinding time and mill rotation rate was variable to account for different process parameters. Time was set at 1 hour initially and in later tests 2 hours of grinding were used to pulverize the material. The precise grinding time was not the subject of this research. The rotation speed was determined based on sound. That is that the mill is accelerated until the sound of ball impacts on the liner are audible. The rotation speed was then decreased until the specific noise is no longer observed indicating that the ball trajectory is landing on the toe of the charge. The ball charge used was 90 balls for the testing necessary in this project. The media Charge was composed of fresh, unused 2.5” balls. This is not representative of a conditioned charge that would normally be expected in a ball mill. It is notable that the non-conditioned charge may affect the process output size.

Ball Mill Procedure:

1. Ball Mill is cleaned prior to use, if additional cleaning is necessary the mill can be run with silica sand for a short time before testing.
2. Lower door should be closed and all 4 bolts should be tight before charging
3. Mill is charged with material

4. Ball Charge is loaded
5. Upper door is closed and all 4 bolts are tightened using a wrench
6. Cage is moved into place to protect operators from the rotating mill
7. Mill is plugged in
8. Mill power switch is switched to the “ON” position
9. Mill rotation is initiated by turning the speed dial clockwise
10. Mill rotation speed is increased until a loud impact sound is heard this is the ball trajectory is impacting the liner
11. Mill rotation speed is reduced until the sound changes to indicate that the ball trajectory is impacting the toe of the charge.



Figure 3.3: Ball mill with shredded hard drive and ball charge.

### **3.1.3 Demagnetization:**

Demagnetization is accomplished thermally by raising the magnetic material to a temperature above the curie temperature which for these magnets is approximately 320<sup>0</sup>C. Magnets with a higher dysprosium content would be expected to have a higher curie temperature. This step also pyrolyzes epoxies found in the HDD including those holding the magnet in the spindle motor and holding the magnet in the magnet bracket as well as melting or pyrolyzing the plastics present in the drive. This demagnetization is carried out in a furnace with airflow and ventilation to a fume hood.

#### Procedure for Demagnetization:

1. Furnace used for demagnetization should be ventilated to a fume hood especially if whole hard drives are to be demagnetized
2. Furnace should have some airflow especially to Demag entire HDDs
3. The charge is loaded into the furnace in a stainless-steel oven pan
4. The furnace is turned on and set to 350°C
5. When the furnace reaches temperature, a timer is set and temperature is held as long as deemed necessary
6. The furnace is turned off and material is left in the ventilated furnace until the charge temperature is below 50°C.

For demagnetization time at temperature was 1 hour at 350°C for whole hard drives this is mostly due to the energy required to heat the internal components of the drive. For manually disassembled magnet assemblies shorter holding times were used (20-30 mins). There was little research conducted on the time at temperature required to demagnetize material. This time at temperature was observed to be sufficient for the purposes of this project.



Figure 3.4: image of magnet assembly before and after demagnetization

### **3.2: Separations Equipment:**

Various laboratory separations equipment were used to evaluate the effect of various separating forces on the material.

These include multiple magnetic separators manufactured by Eriez magnetics. A high intensity and low intensity magnetic drum. The high intensity drum is an Eriez permanent rare earth drum (Figure 3.5 on page 24). The low intensity unit functions similarly but with a smaller magnetic field. Cleaning the drum and in the case of the low intensity unit the surrounding box is necessary as some material will be retained after use. This material can be added back to the magnetic fraction produced. These units are used both for large particle size separations and for upgrading fines.

These drums use a permanent magnet in a fixed position with a drum rotating around that magnet. The feed material is poured over the drum surface in a monolayer, the magnetic material interacts with the magnetic field to adhere to the surface. The nonmagnetic material will fall off the outer edge of the drum due to gravity in front of the splitter, the magnetic material will be held against gravity by the magnet until it leaves the magnetic field, when it leaves the magnetic field it will fall on the other side of the splitter into another receptacle.

Procedure for use of Eriez high intensity rare earth magnetic drum:

1. The door at the bottom of the hopper is confirmed to be closed before loading material
2. Material is loaded into the hopper
3. Plastic receptacles are placed on either side of the splitter on the ground under the magnetic drum
4. The splitter is angled appropriately, the angle of the splitter can affect the grade of the concentrate fraction and the recovery of magnetic material.
5. The unit is turned on including setting the rotation speed of the drum and the feed rate of the vibratory feeder
6. The door at the bottom of the hopper is now removed and feed rate adjusted as observed necessary
7. Particularly when working with fines the contact surfaces must be cleaned off after use, this includes the vibratory feeder and hopper as well as the magnet drum and the frame below the drum. The magnet drum particularly can retain highly magnetic material.



Figure 3.5: Eriez Rare Earth 15 inch drum.

Procedure for use of low intensity magnetic drum (Figure 3.7 on page 25):

1. The receptacle boxes must be removed and cleaned thoroughly before use. Also, the right side of the unit must be cleaned to insure retained material does not pollute the product.
2. The receptacles are placed under the splitter with the skirt laid on the inside of the receptacles
3. The magnetic drum is turned on, this unit features no variability of the splitter or drum speed and must be manually fed.
4. The material feed should be fed at a constant rate as a monolayer to ensure separation.
5. After the machine is switched off the split fractions can be removed in their receptacles.
6. Especially when processing magnet material significant retention was observed in the unit especially on the right side of the box.

Procedure for use of rare earth roll (belt) magnetic separator (Figure 3.6 on page 25):

1. The hopper is loaded with material, material should be  $\frac{1}{2}$ " for this separator
2. The receptacles are cleaned thoroughly before use
3. The belt is turned on
4. Feed rate is adjusted to feed a monolayer of material onto the belt
5. Receptacles are emptied and cleaned with a paintbrush



Figure 3.6: Low intensity magnetic drum separator.



Figure 3.7: Rare Earth Roll magnetic separator

The Davis Tube and rare earth roll magnet are primarily used on fine materials. The Davis Tube allows a variable magnetic field to be used to determine if ferromagnetic fines can be separated from impurities.

This device functions significantly differently than the 3 magnets discussed above. The material is suspended in water by surfactant and added to a glass tube (Figure 3.8). A magnetic field is introduced to hold the strongly magnetic material in the middle of the tube while the nonmagnetic material is washed off. The magnetic field is then shut off and the magnetic material is drained into a second receptacle.

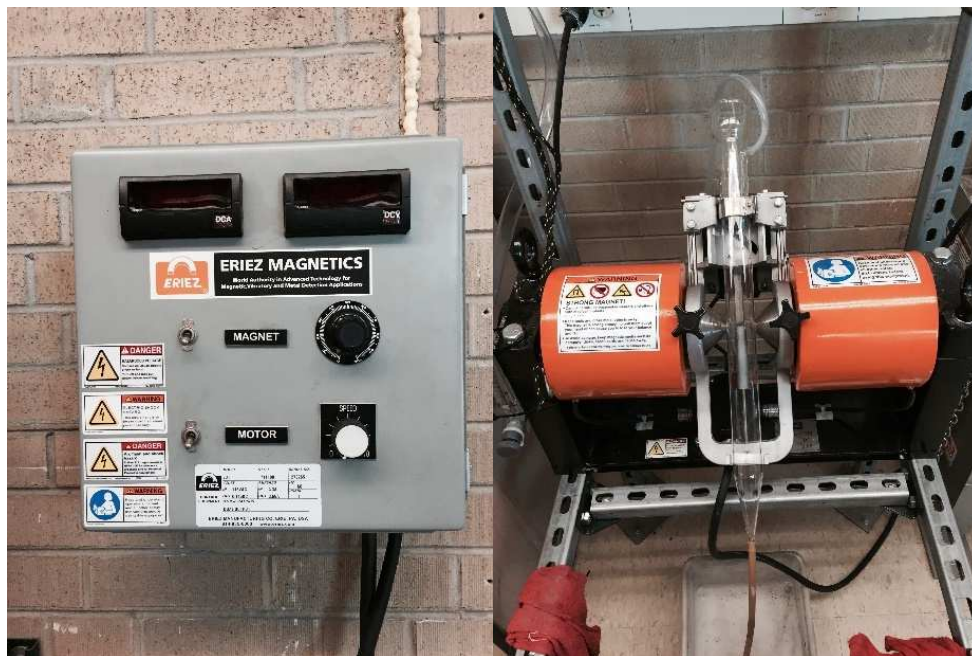


Figure 3.8: Davis Tube and Davis Tube control panel

Procedure for use of Davis Tube:

1. Material must be wetted prior to processing, the procedure for this is in section 1.2.6.
2. The head tank is filled until it is overflowing slightly
3. A receptacle is placed under the spout at the bottom of the Davis tube
4. The valve is opened so that water may flow through the Davis tube, there is a flow gauge between the head tank valve and the tube that can regulate the flow
5. The end of the Davis tube is clamped
6. Wetted material is added to the top of the Davis tube

7. The oscillation is turned on, the magnetic field can be controlled by the control panel. Magnetic field is turned on.
8. The nonmagnetic fraction can be drained through the tube into the receptacle while the magnetic field is on
9. A new receptacle is placed under the spout
10. The magnetic fraction is drained by turning off the magnetic field and allowing the material to flow through freely.
11. The head tank is closed and the feed to the head tank is shut off.

The separations of magnetic from non-magnetic materials are carried out on any of the several magnetic separators discussed above.

It is also possible to separate materials based on difference in conductivity by eddy current separation. This machine features a magnet rotating within a coil of copper wire to produce an electric field at the end of a belt. The electric field induces electric currents in conductive material passing over the belt. If this material is non-conductive it will dissipate the electric field and fall normally. Conductive particles will maintain their own electric field. The primary electric field and the induced electric field will mutually repel and force the particle to the far side of the splitter.

Procedure for use of the Eddy Current:

1. Receptacles are placed under the eddy current on either side of the splitter
2. The eddy current is turned on and belt speed and electric field generator speed are set.
3. Splitter position is set
4. Material is fed by pouring onto the belt
5. During separation the bottom of the belt should be inspected periodically for retained material. Steel in particular can stick to the belt and heat leading to potential melting of the belt.
6. The eddy current machine is shut off before opening and removing the receptacles.



Figure 3.9: Eddy current separator

There were additional separation tests based on density as a separating force. The tools for this testing include several technologies; the shaking table, air table, and vanning plaque. These separators separate based on specific density.

**Shaking Table:** The shaking table is used to separate material of different specific gravities. It requires the material to be sufficiently wetted with surfactant to be suspended in water as it flows over the table. The dense material sinks to the far end of the table (along the axis of shaking) while the low-density material flows over the riffles and exits at the near end of the table.

Procedure for wetting material:

1. Material must be wetted before being separated in a process that uses water. This wetting is accomplished using surfactant
2. Water is added to a bucket
3. Material is added to the water in the bucket
4. The suspension is agitated
5. Surfactant is added in small quantities and agitated in-between additions
6. When the material is suspended in the water it is ready to be separated
7. Best results were obtained by agitating the suspension with an overhead mixer for at least one hour prior to processing.

### Procedure for Shaking Table:

1. Material must be wetted prior to separation, this is accomplished with the procedure above.
2. Buckets are positioned under the splitter hoses for the shaking table to act as receptacles for the separated material
3. Water flow is initiated to the shaking table
4. The shaking table is turned on
5. The material is fed to the table
6. Upon completion of the separation the shaking table motion is turned off and then water flow is closed



Figure 3.10: Shaking Table. The heavy fraction comes off the left side of the table, The light fraction comes off the right side over the ridges.

The air table separates material based on density but the fluid used is air rather than water. Material does not need to be wetted for this device.

1. As there is significant dust generation from this piece of equipment PPE should be worn including a breathing mask. The baghouse should be turned on capture airborne particles
2. Material is added to the feeder hopper
3. Air table is turned on and airflow and table throw speed is set
4. Vibratory feeder is turned on

5. The sample is split such that the low-density material floats over the dividers and ends at the near end of the table, the high-density material will be thrown in the direction of the table motion and exit the far end of the table
6. It is important that the airflow be started lower than expected as material will be lost if airflow is too high



Figure 3.11: Air table density separation equipment

The Vanning Plaque is used to separate material on the basis of density.

Procedure for Vanning Plaque:

1. Material is wetted prior to separation according to the procedure above.
2. Suspended material is added to the vanning plaque which is gently gyrated until some material settles
3. The material that is suspended is poured off the plaque and the settled material is placed into another container
4. This can be repeated as necessary to produce sufficient product in each fraction
5. This can be accomplished with various levels of intensity to produce a cleaner con or tail as desired.

#### **3.2.1.9 Screening and Particle Size Analysis:**

Laboratory screening is accomplished with either of 2 screening devices. The Gilson screen is used to screen larger samples. The Gilson consists of several screens in order of

descending size and finally a tray all mounted in a frame that oscillates to facilitate screening. The purpose of this apparatus is to determine the particle size distribution of a sample. The screen sizes used for analysis of the shredder output was 1.5"-7/8"-3/4"-1/2"-3/8"-4mesh-tray. For analysis of the ball mill output a screen series of 1/2"- 3/8"-4mesh-8mesh-12mesh-16mesh-30mesh-60mesh-tray. This unit is used for most of the screening necessary in the process including the post ball mill screening. There is also a Ro-tap unit used with Tyler screens to determine the particle size distribution of smaller samples. The Tyler screens are also used for wet screening. screening or size classification is a common process step in milling operations. There are 3 pieces of equipment to screen different volumes of material with different process parameters.

The Gilson screen is a 3x1 foot screen deck that can screen material through up to 7 sequential screens. The Gilson has a motorized eccentric that oscillates the screens mounted in its frame to preform separation. There is a tray installed in the bottom of the Gilson to catch the undersize from the final screen. It was found that when screening fines the Gilson could be sealed to improve recovery, This was accomplished by installing a sheet of cardboard over the front and top openings of the Gilson. The screens must be put in and clamped prior to installing the cardboard and sealing. The edges of the cardboard were fastened to the Gilson unit by duct tape and edges were sealed by additional tape. A small door was cut into the lid to allow feed of material while the Gilson was sealed.

Procedure for using the Gilson screen:

1. The screen decks are cleaned prior to use, the frame of the screen decks can retain fine material
2. The screen decks are loaded into the Gilson unit and clamped into position.

Steps 3-6 are optional

3. 2 pieces of cardboard are cut. One such that it covers the front opening of the Gilson, and one such that it covers the top opening of the Gilson unit.
4. The two pieces are installed by holding the cardboard over the opening and sealing the edges with duct tape.
5. A small hole (3x5 inches is recommended) is cut into the top cover using a knife. Only 3 sides of this square should be cut such that the 4<sup>th</sup> side can operate as a hinge.

6. The hinge mentioned in step 5 and any other cracks in the cardboard are sealed with duct tape. Particular attention should be paid to the back of the to cover to ensure that the holes around the shocks are as small as possible.
7. The material is loaded onto the top screen in small increments to prohibit blinding of the first screen. Oscillation is started by switching the Gilson unit on once it is plugged in.
8. Personnel should stand on the Gilson screen feed to keep it from moving
9. Material is added incrementally as necessary, it may be necessary to remove and empty screens if they become overloaded during screening.
10. To empty the unit screens are removed and dumped into a wide receptacle. with metals it is often necessary to force the material back through the screen holes as the material can twist onto the screen grate.
11. When screening fines the screens should be impacted on the floor (in a container) such that the material entrapped in the cracks can be recovered.



Figure 3.12: Gilson screen (left) with screens installed. Dust cover installed (right) with air draw to bag house visible at bottom of the image.

#### Tyler screens:

The Tyler screens are 8-inch screens with a brass case around a mesh screen. They are commonly used for particle size analysis. Several such screens can be arranged in a stack with a pan and a lid on either side and used in a ro-tap unit. This allows rapid screening of a sample

through the screen stack as desired. Tyler screens are also used for wet screening of material using a sink sprayer and a fixture that fits over a 5-gallon bucket.

Procedure for use of Tyler screens with Ro-tap unit:

1. Screens are cleaned prior to use, fine screens in particular can be cleaned by flowing water backwards through the screen. It is also possible to clean with compressed air in the same manner. Screens, particularly fine screens, should be inspected for holes prior to use as holes can affect the results of particle size analysis
2. The screens must be thoroughly dried after cleaning
3. The screens are stacked in descending order; that is the coarsest screen, the smallest Tyler sieve number, is at the top, and the finest screen associated with the largest sieve number is in the bottom of the stack.
4. A pan is fitted to the bottom of the stack
5. Sample is added to the top screen
6. Lid is installed at the top of the stack
7. The stack is loaded into the ro-tap unit and timer is set, upon pressing start the unit will rotate and tap the screen stack to facilitate screening
8. After the timer ends the ro-tap will automatically stop and the stack can be removed
9. The screens are removed one by one starting with the coarsest size and the oversize is dumped into a receptacle
10. Screens should be cleaned after use to ensure recovery and prepare them for the next user.

Procedure for wet screening

1. Necessary Tyler screen is cleaned and inspected for holes. The cleaning can be accomplished by countercurrent flow of water through the screen opposite to the normal direction of material.
2. The fixture is placed over a 5-gallon bucket
3. Tyler screen is placed in the fixture such that the undersize material will flow through the screen into the bucket
4. Material is loaded onto the screen; this material can be dry or a slurry
5. The sink sprayer is used to wash the undersize through the screen
6. Upon completion of screening the screen oversize is dumped into a receptacle

7. A finer screen can be selected and a new 5-gallon bucket placed under the fixture. Steps 1-6 can be repeated as necessary.



Figure 3.13: Ro-tap screen stack.

### 3.3: Analytical Procedures and Tools:

Analysis of both feed materials and products has been completed by several analytical tools at the Colorado School of Mines and at Hazen Research. XRF is used initially for indications of success but the inability to demonstrate reliability of the XRF instrument has limited the results of this research to be based upon ICP-MS and ICP-OES results rather than XRF.

XRF is used to analyze the outputs for initial grade and recovery calculations. XRF analysis is advantageous due to its short sample preparation procedure and rapid testing time. Powder pressed XRF samples are prepared with 90% sample 10% boric acid binder mixture. Fused glass XRF samples are prepared with 0.21g of sample with 10.29g of lithium borate. The pressed or fused sample is scanned by XRF using the Uniquant method, initially. Uniquant is a standardless analysis method with limited precision and accuracy. Using standards with similar matrices to the expected process material a method can be programmed into the analysis software for more accurate results.

Standardization for this research was to be completed manually with a standardization curve developed from spiked samples matching the expected matrix of the process output. Scan results were produced from the Uniquant method. There are 2 sets of standards used for this analysis. 4 standards are prepared of each set. The compositions of these standards are shown in table 3.1.

Table 3.1: Stanardization sample compositions with known amounts of added oxide. MGBM samples are based on process output and XRF samples are based on a ground pure magnet. 4 samples are spiked with neodymium oxide and 2 samples with silica.

Sample	Total mass	Mass of Process material	Mass of Oxide
XRF +0	0.2098	0.2098	0.0000
XRF +5	0.2206	0.2099	0.0107
XRF +10	0.2312	0.2102	0.0210
XRF-5	0.2205	0.2098	0.0107*
MGBM 0	0.2100	0.2100	0.0000
MGBM +5	0.2099	0.1994	0.0105
MGBM +10	0.2100	0.1890	0.0210
MGBM -5	0.2102	0.1996	0.0106*
* prepared with SiO <sub>2</sub> in place of Nd <sub>2</sub> O <sub>3</sub>			

The first set of samples is based on a spiked Nd<sub>2</sub>Fe<sub>14</sub>B magnet with added 99.9% pure Nd<sub>2</sub>O<sub>3</sub> or 99.5% pure SiO<sub>2</sub>. The results of these scans are shown in blue in figure 3.14. The second set of samples are based on a spiked sample of process output with known additions of Nd<sub>2</sub>O<sub>3</sub> and SiO<sub>2</sub>. The results from these standards are displayed in orange in figure 3.14. These prepared samples were retested several times without modification to determine the measurement uncertainty of the XRF. The results are tested using a Dixon's Q-test to statistically rule out points that represent departures from each data set.

$$Q = \frac{Gap}{Range} \quad (3.1)$$

$$Q \geq Q_{critical} \rightarrow \text{Data point is erroneous}$$

Q critical is dependent on the number of data points in the data set and the confidence interval. For the elimination of points in this analysis a confidence interval of 90% was used for  $Q_{critical}$ . This test is based on the quotient of the difference between the outlier and the next furthest point divided by the range of the sample set. There is a critical value based on a confidence interval and the number of data points in the set. The results of the XRF scans on the samples from table 3.1 are shown in figure 3.14.

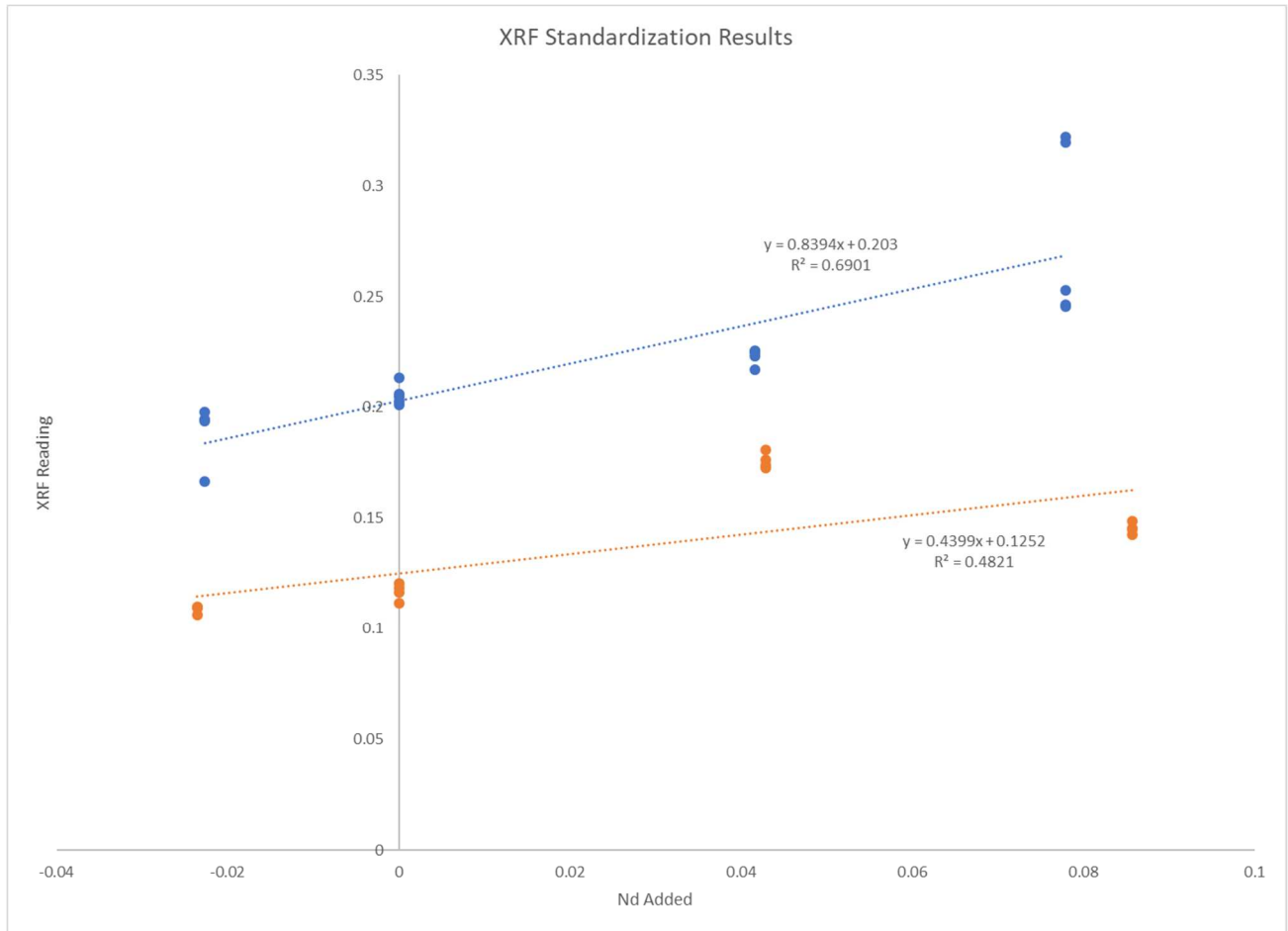


Figure 3.14: Results of XRF scans on standards.

The results of these XRF standardization leave significant questions about the expected precision and accuracy of this analytical methodology. There are concerns about both the precision and accuracy of this data, the repeated scans for each sample were conducted without modification or any contact with the sample. There is not sufficient correlation between the results of these standards to plot an effective standardization curve. The failure of this data to

show correlation between increased neodymium composition and increased XRF reading evidences that XRF results are not sufficient for conclusions. It is suspected due to the fact that repeated scans of the same sample without modification return significantly different results that the error is with the XRF instrument itself. Due to this the conclusions made for process results are not based on XRF results.

Procedure for Pulverizing material (Figure 3.15):

1. The ring and puck pulverizer is thoroughly cleaned internally before use
2. The material is filled in between the ring and puck and/or between the ring and outer vessel of the pulverizer
3. The rubber gasket is placed evenly on the top of the pulverizer vessel and the lid placed ontop of that gasket
4. The entire vessel is placed in the pulverizer unit and clamped
5. The material is typically run for on the order of 10 mins but this is variable based on volume of material and initial particle size
6. Material is removed by dumping out the pulverizer vessel and brushing off the internals, the ring, and the puck to recover all the material present.



Figure 3.15: Pulverizer for fine grinding of XRF samples.

Procedure for XRF pressed sample preparation:

1. Representative sample is pulverized to roughly 325mesh and below, this is monitored by grind time rather than actual particle size.

2. Sample material is combined with boric acid by mass with recommended ratio of 9:1, Higher ratios of boric acid are sometimes used when the initial sample procedure produces an incoherent sample. Samples are prepared with 9 grams of sample material and 1 gram of binder initially.
3. The mixed material is added to an XRF sample sleeve and then placed into the ram of the isostatic press.
4. The sample is loaded in the isostatic press and pressed at 30psi for 2.5 mins.



Figure 3.16: Press used to prepare XRF samples.

Procedure for XRF fused sample preparation:

1. Representative sample is pulverized to roughly 325mesh and below, this is monitored by grind time rather than actual particle size
2. Prior to use for the day it is suggested that the Pt crucible be cleaned with a barren charge of lithium borates to dissolve any contaminants
3. 0.21g of sample is massed and added to 10.29g of lithium borates. The specific lithium borate chemistry used is dependent on the sample chemistry.
4. Mixed sample is placed in the fluxer's platinum crucible and the appropriate furnace schedule is selected for the sample chemistry
5. The sample is removed from the mold, If sample is not intact it can be re-melted and fusion can be attempted again

6. It is recommended that the platinum crucible and the mold be cleaned thoroughly on a regular basis. The platinum crucible can be cleaned by running clean lithium borates (no sample material) through the same method being used for sample preparation. The



Figure 3.17: Fuser used for preparation of fused samples.

maximum lithium borate amount that can be cast in the mold is 10.5 grams as additional material may overflow the mold. This is the maximum that should be used for cleaning.

Procedure for XRF sample analysis:

1. Sample is loaded into XRF sample bank
2. XRF analysis program is selected
3. Green “play” button is pressed on the computer program
4. Results can be saved as a pdf or xcel file

ICP-MS is used for quantitative elemental analysis of aqueous material. Solid samples of interest must be digested in an acid solution to produce an aqueous sample. Aqueous digestions are sampled and diluted to reduce the total dissolved solids concentration to below 1ppm. The ICP’s sampling arm robot can carry out a dilution of up to 100:1 so samples must be prepared below 100ppm before the ICP and its associated machinery can analyze them. Five standards are prepared for the ICP-MS standardization from stock standards diluted to five different levels of total dissolved solids. Standards were also produced by spiked magnet powder samples and spiked process output samples the same as those discussed above for XRF standards in order to determine the effect of interference between the various rare earths present. Only 3 standard samples were used for the ICP standardization with the silica diluted sample not being used. The

results of these standard samples for both ICP-MS at CSM and ICP-OES at an outside laboratory are shown in figure 3.18.

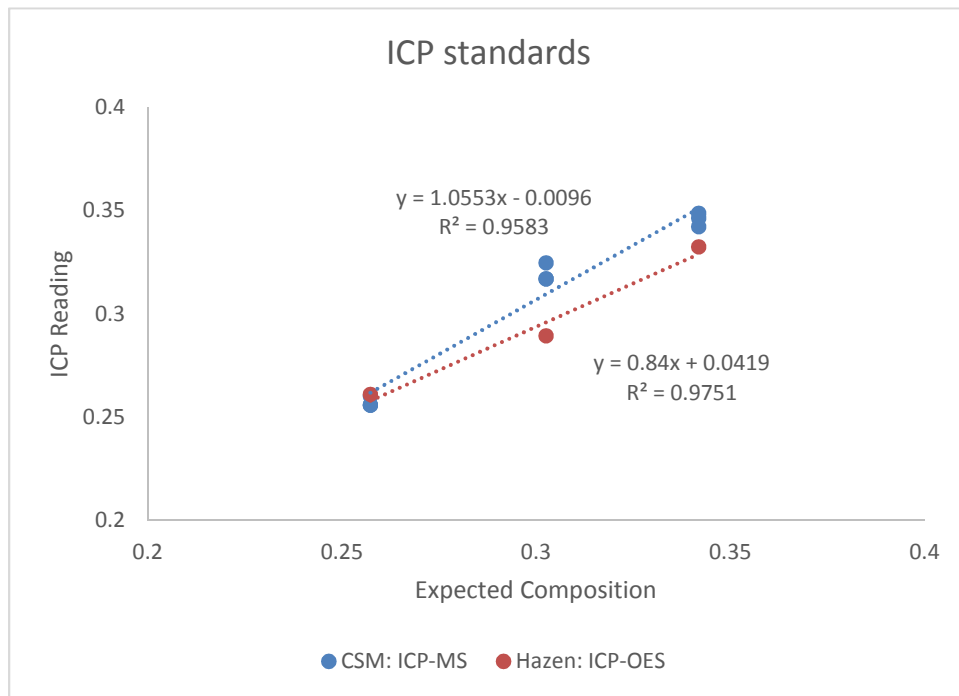


Figure 3.18: Standardization Curve for ICP-MS results

The results for the ICP-MS were run in triplicate producing 9 different results at 3 expected compositions. The Slope of this line represents the change in reading (vertical axis) as a function of the change in sample composition. This slope should be 1. The intercept represents a consistent, systematic, error in the reading. The data shows that ICP-MS is somewhat more accurate with regard to measuring neodymium than ICP-OES, this is expected as rare earth masses are expected to cause less interference than optical spectra.

ICP-MS sample preparation procedure: digestion by nitric acid

1. Sample is massed precisely as this is necessary to ensure accuracy in analysis of ICP data
2. All glassware is cleaned prior to digestion
3. Deionized water is added to the clean reaction vessel
4. Nitric acid is added to the water in the reaction vessel
5. Sample is added to the nitric acid mixture in the reaction vessel

6. Sufficient time is allowed for the sample to react and fully digest. This often means leaving the sample overnight
7. The sample is filtered using a grade 40 filter paper
8. The filtered sample is diluted to 1L using deionized water
9. The 1L sample is diluted further as discussed below.

#### ICP-MS Sample preparation procedure: digestion by Aqua Regia

1. Sample is massed precisely as this is necessary to ensure accuracy in analysis of ICP data
2. All glassware is cleaned prior to digestion
3. Hydrochloric and nitric acid are measured out by volume, the ratio should be 3:1 Hydrochloric to Nitric.
4. Nitric acid is added to the reaction vessel
5. Hydrochloric acid is added to the reaction vessel
6. Sample is added to the aqua regia mixture in the reaction vessel
7. Sufficient time is allowed for the sample to react and fully digest. This often means leaving the sample overnight
8. The contents of the reaction vessel are poured into a vessel containing approx 300ml of water.
9. The sample is filtered through a grade 40 filter paper
10. The filtered sample is diluted to 1L using deionized water
11. The 1L sample is diluted further as discussed below.

#### ICP-MS dilution procedure:

1. The necessary dilution is estimated using the known sample mass that is dissolved in the litre of sample. The ICP-MS requires an input below 1ppm total dissolved solids but the dilution robot can dilute up to 100x. Therefore, the dilution must reduce the dissolved solids amount to below 100ppm
2. The scale is tared with a 50ml sealable vial
3. the 1L sample prepared by digestion above is sampled using a pipet.
4. This is added to the empty 50ml vial
5. The mass is recorded and the necessary diluent volume is determined
6. The sample is tared again
7. The sample is diluted using analytically pure 2% nitric acid solution.

8. The mass of added diluent is recorded

All process inputs and outputs were analyzed in replicate including multiple samples analyzed by various methods in house (ICP-MS and XRF) and an additional split from each was analyzed at Hazen Research using ICP-OES. It was confirmed that Hazen's ICP-OES and CSM's ICP-MS are found to agree by analyzing splits of the same process output on both machines.

Standard development for analytical tools:

Previously developed standards for Nd-Fe composition analysis for other research projects were used initially for analysis. Later standards were developed using known quantities of Nd<sub>2</sub>O<sub>3</sub> mixed with magnet powder. The standards were used to determine the accuracy of both XRF and ICP-MS. It was found that particularly for the XRF analysis the matrix composition can affect the readings to a large degree therefore efforts were made to match the expected matrix as closely as possible when preparing known standards, this allows the matrix effect to be controlled. ICP-OES also exhibits some interference between the various rare earths so by matching the matrix of the standards to the unknown material the interference can be accounted for.

Fire Assay:

Fire assay is a technique developed originally during ancient times for determining the amount of precious metals in a sample of material. Generally, this is accomplished by a 2-step process of fusion and cupellation. In the fusion step the material to be assayed is added to a lead oxide mixture along with flour. The flour reduces the lead oxide into liquid lead which dissolves the precious metals in the sample. This liquid lead phase containing the precious metals is cast and then melted in a cupel to produce a mixed precious metal bead. The procedure is as follows:

Procedure for Fire Assay:

1. Flux is mixed including lead oxide, silica, and flour. The exact composition is dependent on sample chemistry.
2. Flux is added to a sample of material and mixed together in a crucible
3. Crucible is placed in a furnace and heated to 1000°C. After 1 hour at temperature this material is cast in an Iron mold.
4. The lead casting is hammered into a cube
5. The cube is placed on a cupel and that cupel is placed in a furnace

6. When the lead begins to melt the airflow in the furnace is turned on to oxidize the lead
7. The furnace is held at temperature with airflow until all of the lead is adsorbed by the cupel
8. The cupel is removed from the furnace with a bead containing the precious metals in the depression. The lead will have oxidized and been adsorbed by the bone ash cupel

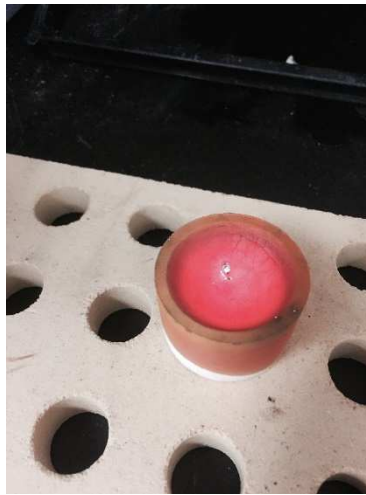


Figure 3.19: Fire assay bead in cupel.

### 3.4 Determination of Head grade

Head grades are determined by manual disassembly of hard drives including demagnetization to allow liberation of the magnet from the magnet assembly. An additional bonded magnet is removed from the spindle motor assembly, upon demagnetization of the spindle motor the epoxy that holds the magnet in the motor is decomposed such that the magnet can be easily removed. The whole of both of these magnets are digested using aqua-regia and diluted for ICP-MS analysis. The ICP-MS is used to determine the composition of these magnets. The head grade is then calculated using the ICP composition and the mass fraction of magnet material in the disassembled hard drive.

The magnet material is tracked through the various process steps by quantitative analysis of the neodymium composition.

The organic fraction of outputs is believed to be composed mostly of printed circuit board materials broken up upon milling. This fraction is measured by loss on ignition testing (LOI). Loss on ignition is completed according to ASTM D7348-13 Method B holding samples at 950°C for 1 hour.

### Determination of Metal Fraction Composition:

The composition of oversize fractions is analyzed and used to calculate recovery and grade for aluminum, carbon steel, stainless steel, nickel alloy, and printed circuit boards. This analysis is completed by sorting each fraction by hand and massing the components as part of each fraction. The grade is approximated by the relative composition of each fraction. That is the grade is represented as the mass of each material as a fraction of the total mass in the stream. The sortation can be visualized in figure 3.20. The 2 aluminum grades, Steel, stainless steel, copper, PCB, and plastic are readily identifiable and can be easily sorted into separate groupings. The limitations of this approximation are user caused, mostly that non-liberated materials can be



Figure 3.20: Sorted metals from shredded hard drive.

challenging to sort. By performing this sortation on process output value streams, it is possible to determine the recovery to said fraction of the material specified.

### Economic analytical procedures:

There was additional analysis completed to determine the head grade for the process. This is completed by disassembling and sorting components by material. Magnet amount is contained in the spindle motor magnet and the reader head magnet. The aluminum is found primarily in the case and the platters, the nickel is found in the magnet bracket, the stainless steel is found in various internal components including the spindle motor and hardware, finally the carbon steel is found primarily in the server bracket and the hard drive case.

Sorting and massing the various components by material of construction allows analysis of the material value encased in hard drives. The magnet material is removed from the spindle motor and reader magnet assembly upon demagnetization.

Economic analysis of hard drive value to support literature determinations was conducted as part of this project. The average HDD composition and mass is determined by the weighted average of occurrences in a 4300 HDD lot counted at partner Oak Ridge National Lab (ORNL). The analysis included disassembly of 26 hard drives.

Material values are determined based on quotes from recyclers for the metal process outputs. This value is discounted to represent uncertainty. The value of circuit boards is determined by pyrolyzing, crushing, and grinding to make a fire assay sample. By fire assay the precious metals composition of the ground circuit board is determined. The total entrained gold and silver value is discounted to 35% to represent the processing cost. This result helps to narrow the range of literature values for the value of circuit boards.

Statement on outside checks for analytical results:

Analytical numbers were confirmed by outside analysis in as many cases as possible. Hazen Research is an analytical lab that completed all of our fire assay analysis as well as performing check assay via ICP-OES. Various CMI partner laboratories also performed analysis on process outputs via a range of analytical methods. These methods included atom probe EBSD at ORNL,

## CHAPTER 4: RESULTS AND DISCUSSION:

### 4.1: Analysis of Head Grade

The analysis of magnet material in the hard drive feedstock includes disassembly to determine the mass of magnet present as well as digestion and analytical chemistry to determine the neodymium present in that material. This disassembly and composition analysis are replicated to determine the deviation in neodymium amount in a hard drive.

Table 4.1: Table of several disassembled Hitachi Deskstar HDDs used to compute the head grade of the process.

Sample	Mass of HDD	Mass of Magnet Assembly	Mass of Magnet	Magnet Wt% Nd	Head Grade
1	849	76.8	22.1	27.5	2.6%
2	850	81.9	22.1	27.7	2.6%
3	844	81.3	22.1	27.5	2.6%
4	848	81.9	22.1	27.8	2.6%
5	844	81.0	21.7	27.6	2.6%
AVG	847	80.6	22.0	27.6	2.6%
STDEV	2.5	1.90	0.14	0.13	0.00

The magnet material is tracked through process steps by measuring the neodymium (associated with the magnet material) in the process flows. The range of neodymium compositions of the magnets is used to calculate the average composition of the feed. It is found that the spindle motor magnet (the red ring in figure 2.8) has a lower concentration of neodymium along with higher iron, higher praseodymium, and lower dysprosium. The neodymium composition of this magnet is 26.1898%. Dysprosium is reduced from about 1.34% in the reader head magnet to 0.015% in the spindle motor.

### 4.2: Behavior of Shredder Output:

The goal of this project was the creation of a process that would recover rare earth magnet material by taking advantage of shredded hard drives as a resource. The initial experimentation was a study of shredder outputs from various shredders. Samples were shredded representing 7 shredders from 4 manufacturers. The analysis of shredder outputs was completed to understand the liberation of magnet material from the shredder crushing step. The first analysis of this material was a particle size distribution analysis determined by screening using

the Gilson screen with screen sizes  $>1\frac{1}{2}$ ";  $-1\frac{1}{2}$ ",  $+7/8$ ";  $-7/8$ "  $+3/4$ ";  $-3/4$ "  $+1/2$ ";  $-1/2$ "  $+3/8$ ";  $-3/8$ "  $+4$ mesh;  $-4$ mesh. The results from this analysis are shown in figure 4.1.

The magnet material is expected to have a better chance of liberation with finer particle size output. This liberation is important for the recovery of magnet material in subsequent unit operations. The shredder output is analyzed to determine the optimal shredder output contributing to liberation of magnet material. Several of the returned samples from manufacturers were significantly (10%) lighter than originally shipped. There is no explanation for this mass loss. The exact procedures for shredding are mostly unknown as limited contact was had directly with the respective manufacturers. The range of  $P_{80}$  sizes was  $5/8$  inch to  $1\frac{1}{2}$  inches.

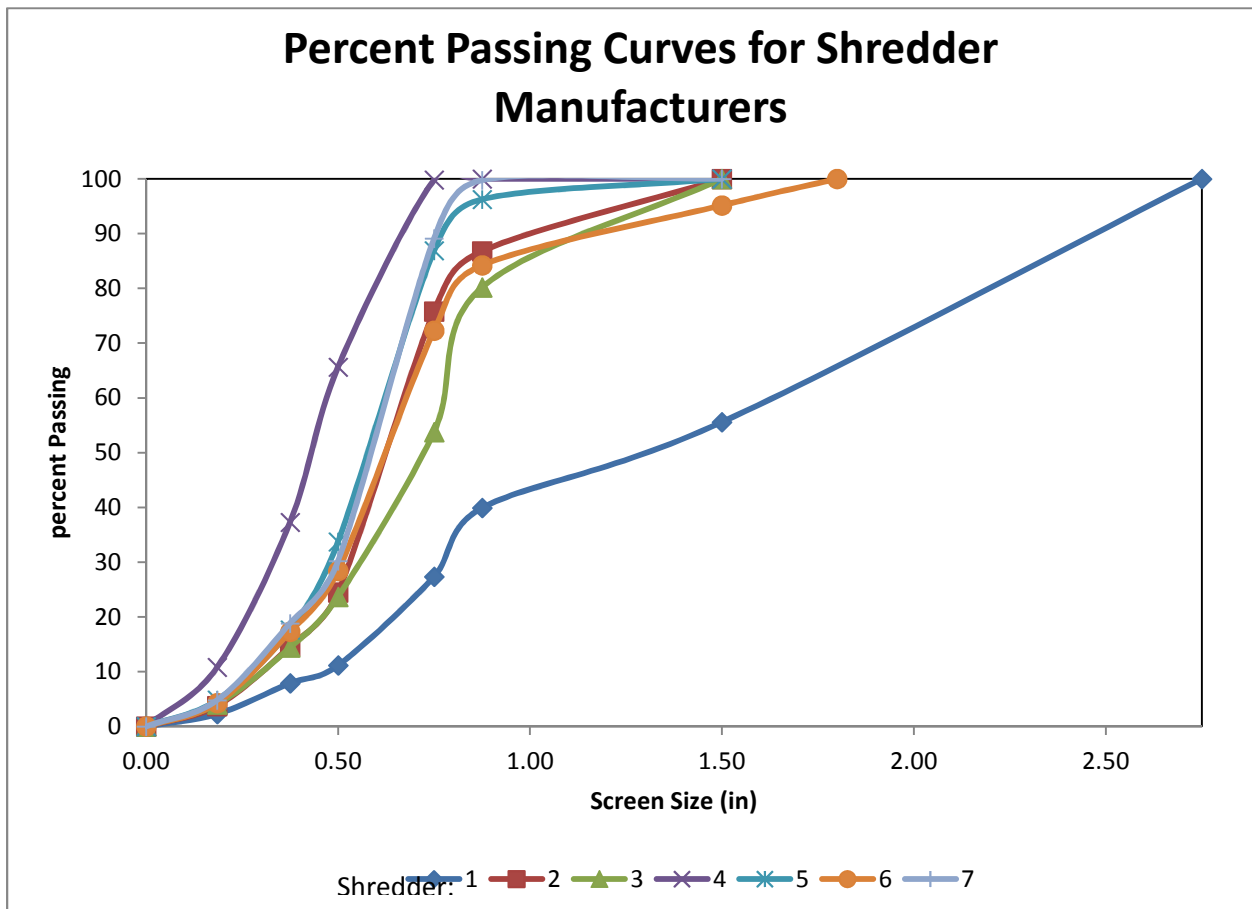


Figure 4.1: Percent passing curves for the shredder output from several shredder

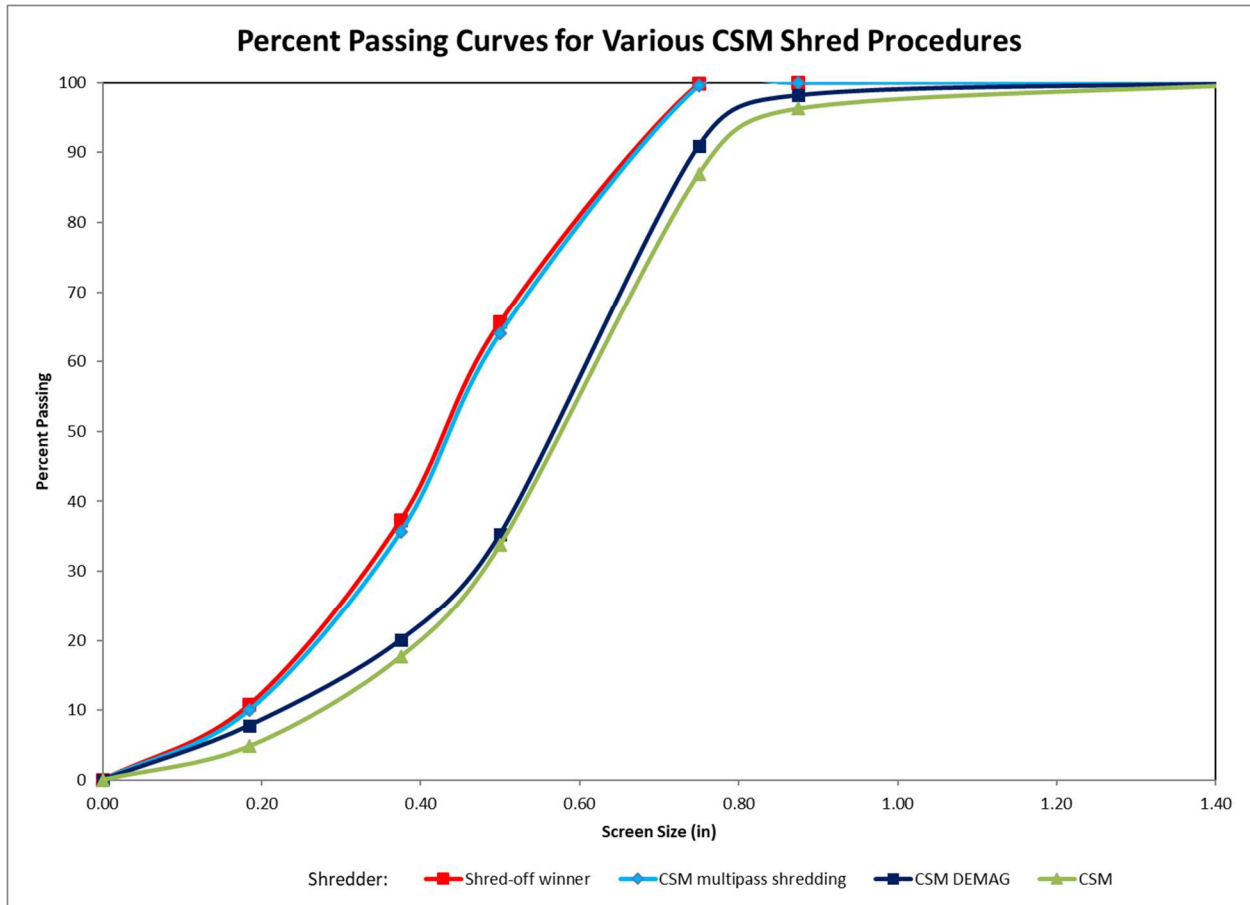


Figure 4.2: Shredder particle size analysis for several variations of shredding procedure including multi-pass shredding and the effect of demagnetization before shredding.

The best demonstrated shredder output attempted to be duplicated by multi-pass shredding using the laboratory shredder installed at Colorado School of Mines. It was shown that that shredder output could be duplicated via 3 shredder passes. The output size distribution was also determined for demagnetized hard drives being shredded.

The shredder comparison experiments were initiated prior to demagnetization experiments and so none of the samples shredded by outside manufacturers were demagnetized prior to shredding. The additional shredder research with results displayed in the figure 4.2 showed that demagnetization can affect the output particle size distribution with a decrease in  $P_{80}$  from  $\frac{3}{4}$  in. to  $\frac{11}{16}$  in. It should be noted that, as expected, demagnetization significantly reduced the observed material retention on the shredder internals.

The various shredder outputs were also processed by drum magnetic separators as a proxy estimate of the liberation of magnet material from the hard drive. The shredder with the finest particle size output also had lower total magnetic fraction representing greater liberation of magnetic material from the nonmagnetic hard drive construction.

Additional analysis of the shredder product included manual separation of identifiable magnet material from screened fractions of the shredder output to determine if magnet material could be concentrated directly out of the shredder. The results of this work are shown in table 4.2.

Table 4.2: Magnet particles found in various screen fractions by hand sortation.

Particle Size:	Identified Magnet Mass:	Distribution Wt%:
-3/4 + 1/2	0	0
-1/2 + 3/8	0	0
-3/8 + 4mesh	19	22.4
-4mesh	66	77.6
Feed	85	100

The results of this analysis showed that magnet material tended to be concentrated in the shredder output as a fraction of particle size, there was no magnet material identified in the +3/8” fraction. However, there remained significant unliberated material that did not lend to effective separation. This lead to additional comminution experiments as discussed below.

### 4.3: Preferential Degradation Theory and Discussion:

Nd<sub>2</sub>Fe<sub>14</sub>B is an intermetallic compound that exhibits brittle fractures when loaded mechanically. This can be observed in the shredder output. When subjected to shearing forces the magnet material shows a characteristic brittle fracture surface. It is expected that a magnet would fracture readily under impact due to this observed brittle nature. A simple experiment was designed to test this expectation by impacting a large piece of magnet material on an anvil using a hammer. The observed result is that the magnet breaks down quite easily upon impact.

It is worth note that ceramic materials such as this intermetallic magnet compound are known to fracture without experiencing plastic deformation. Metals have a different behavior experiencing large plastic strains before fracture. It is expected from this test that the brittle fracture of magnet material can be achieved by impacting the mixed shredder output consisting of magnet material and metals. It is expected in this operation that magnet material can be

degraded preferentially while the metals remain at large particle sizes exhibiting mostly plastic deformation rather than fracturing. This would allow concentration by screening the impacted output to separate the fractured magnets from the metals.



Figure 4.3: Results of magnet hammering experiment.

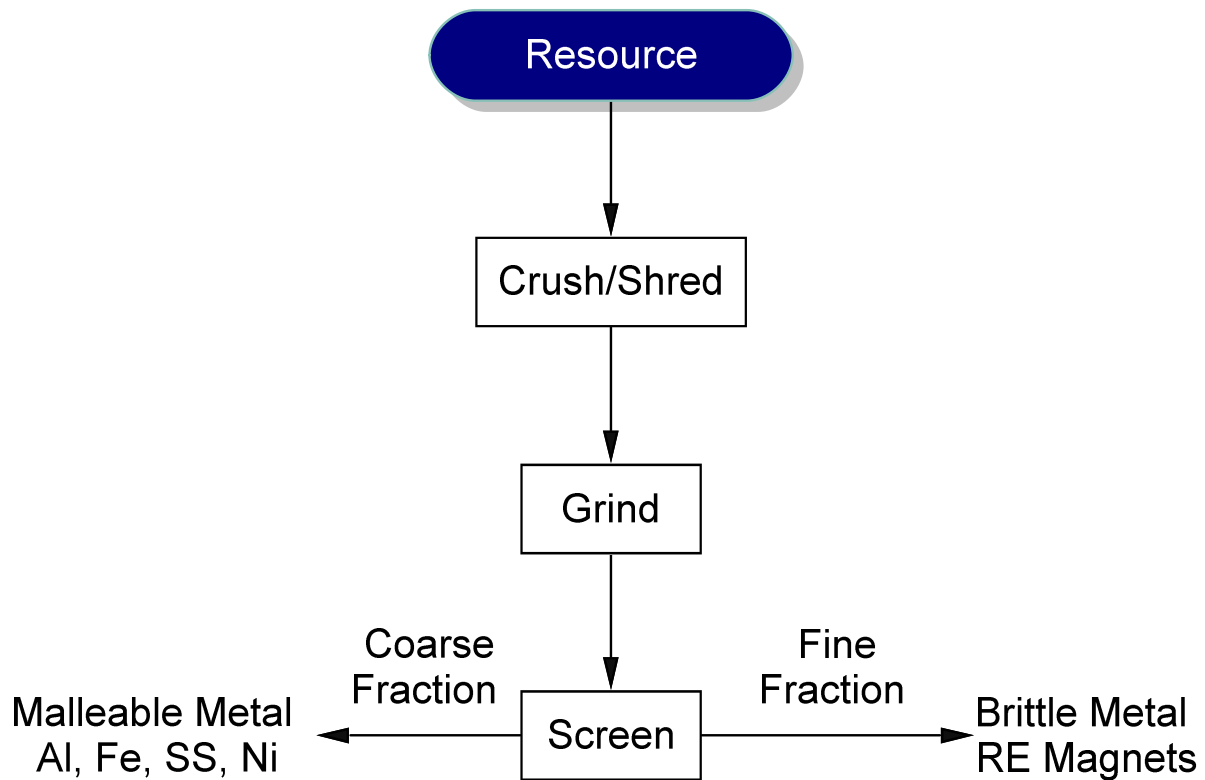


Figure 4.4: Concept preferential degradation flowsheet

This concept of size reduction of magnet material by impacting the heterogenous shredder output is called preferential degradation for the purposes of this paper. The concept is that the preferentially degraded material can be screened to separate a magnet material concentrate. The screen oversize would contain the nickel, stainless steel, carbon steel and aluminum materials while the undersize would include the crushed magnet material and ground circuit board material. Both of these fractions could be further processed to produce economic products.

The repeated impacts necessary for preferential degradation were to be achieved using a ball mill.

#### **4.4: Initial preferential degradation flowsheet:**

Initial experimentation of the preferential degradation flowsheet consisted of testing a 40-hard drive sample. This sample was processed by the 1m ball mill. That ball mill feed was screened to reject material of a size fraction believed to be barren. The screen size was selected from the above handpicking of magnet material from screened fractions. (section 4.2). The sample showed that preferential degradation by ball milling could be achieved degrading the magnet material to a finer grain size than the malleable metals. The fine product was analyzed for composition. Magnet material recovery was shown to be 95%. With a grade of 35% magnet material by weight. This is considered in relation to the feed (head) grade in the hard drives. This represents a significant upgrade by screening as well as liberation of magnet material. The analysis was accomplished by splitting the ball mill output and performing XRF analysis of one of the splits. Whole hard drives were demagnetized prior to shredding and screening to minimize

material hang-up in the processing equipment, hang-up was especially a concern in the steel ball mill.

The ball mill output oversize was separated into several size fractions, the smaller of which were further ground in the laboratory jar rod mill. It was found that significant additional magnet material was retained in these fractions that had not been sufficiently pulverized to pass the 30-mesh screen. The recovery from additional grinding of these fractions is added to the total recovery but further tests were designed to pulverize material further as a result of this study.

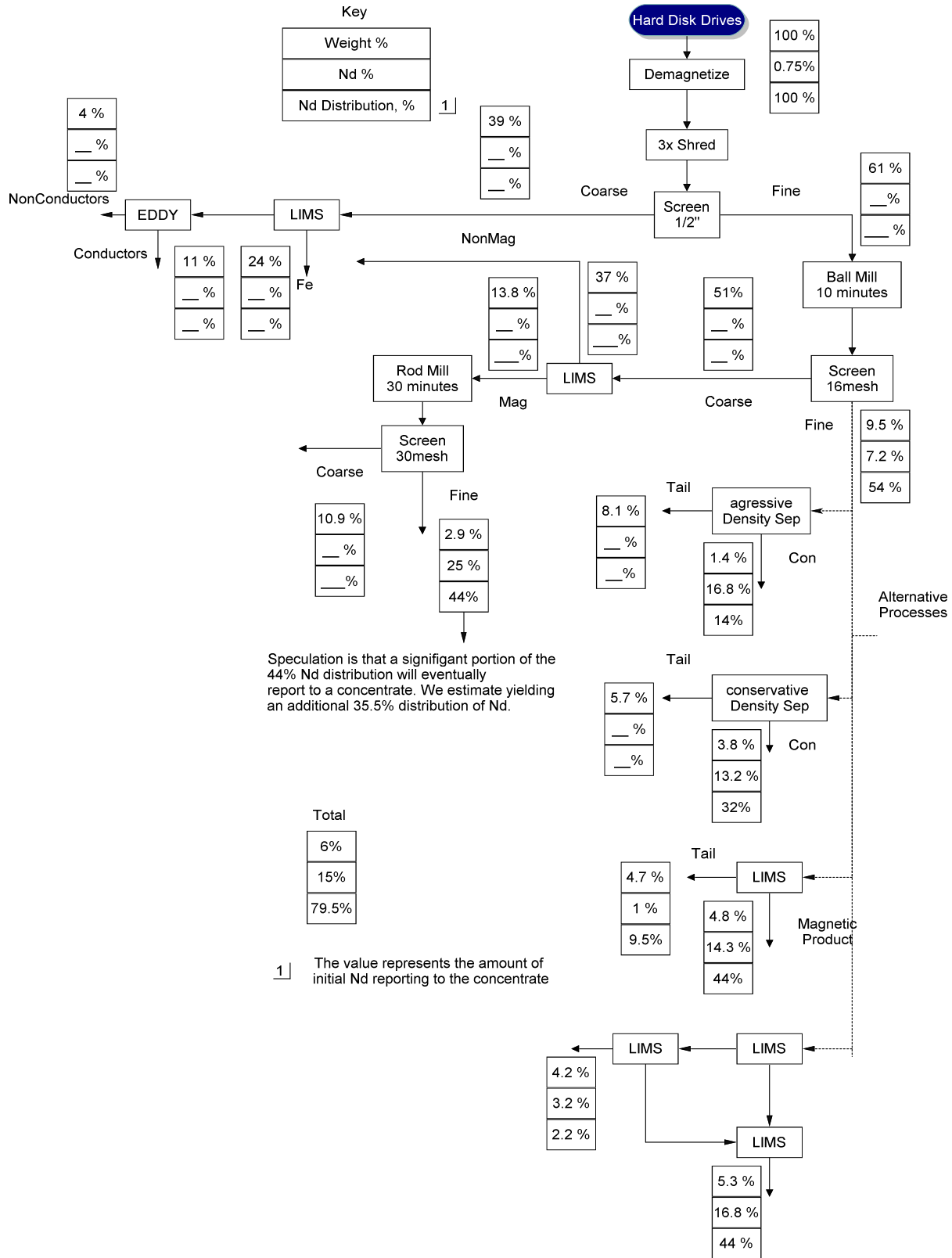


Figure 4.5: Initial screened preferential degradation flowsheet

The undersize output splits were used for testing various additional unit operations for increasing the output grade. These included separations based on density, magnetic behavior and electrical conductivity.

Table 4.3: Table of upgrade studies on ball mill output.

Sample	Input Magnet Grade	Method	Magnet Material Grade in Output	Recovery of Magnet Material
1	32%	Density	47%	59%
2	32%	RE drum	18%	46%
3	32%	Density	59%	28%
4	32%	LIMS	51%	81%
6	32%	beltmag	25%	60%
7	32%	Mag Circuit	59%	79%

The result of the upgrade study shows that magnet material is liberated from the ball mill grinding operation, additional grinding was not necessary to produce a higher-grade output. This research gives evidence that influenced later research direction by identifying the separation forces that may be useful in separating the magnet material from expected diluents. The rare earth drum and rare earth roll magnet separator both showed low recoveries and low concentrate grades. It is expected that these separations methods retained within the process equipment large amounts of high grade material, The LIMS unit retains material as well but is relatively easy to clean out to recover material. This may be due to re-magnetization of the magnet material causing losses as the material attaches to the metal frame of the unit. It is also expected that material remains on the drum or belt even after attempts to clean those pieces of equipment. The magnet circuit utilizes the same low intensity magnet unit arranged such that a cleaner and scavenger unit operation are completed. This flowsheet is visible in figure 4.5.

The results of this study indicate that low intensity magnet separation and density separation are potentially useful for treatment of the process outputs to ultimately produce a higher-grade product.

It was discovered by hand picking that significant magnet material was present in the oversize fraction of the ball mill input. The results influenced further research on a non-screened ball mill feed. This variation of the process was designed to maximize recovery of magnet

material compared to the screened ball mill process. In this variation the entire shredder output is fed to the ball mill and ground. The process flowsheet for this is shown in Figure 4.5

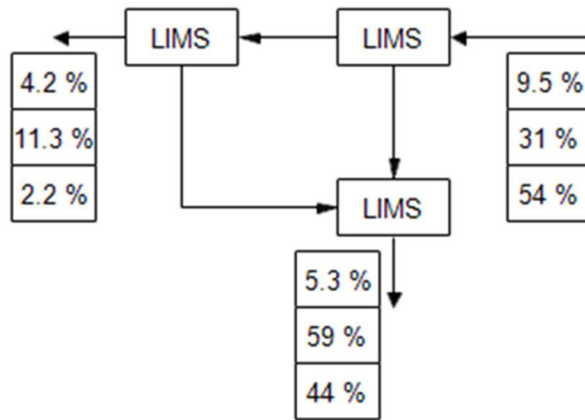


Figure 4.6: Magnetic circuit for upgrading of process output.

The outputs of these 2 processes are analyzed further to determine the composition and material liberation of the undersize output. This analysis included splitting the process output for analysis by both wet and dry screening. The results of this show the true particle size distribution of the fine process output. It should be noted here that upon exposing the magnet material to water the material readily clumps up exhibiting strong hydrophobic behavior.

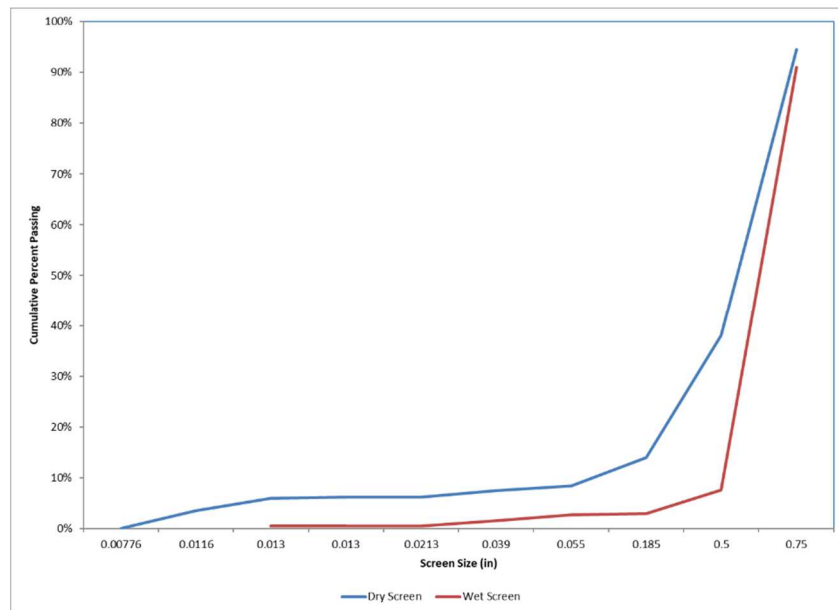


Figure 4.7: Wet and dry screening analysis of preferential degradation process

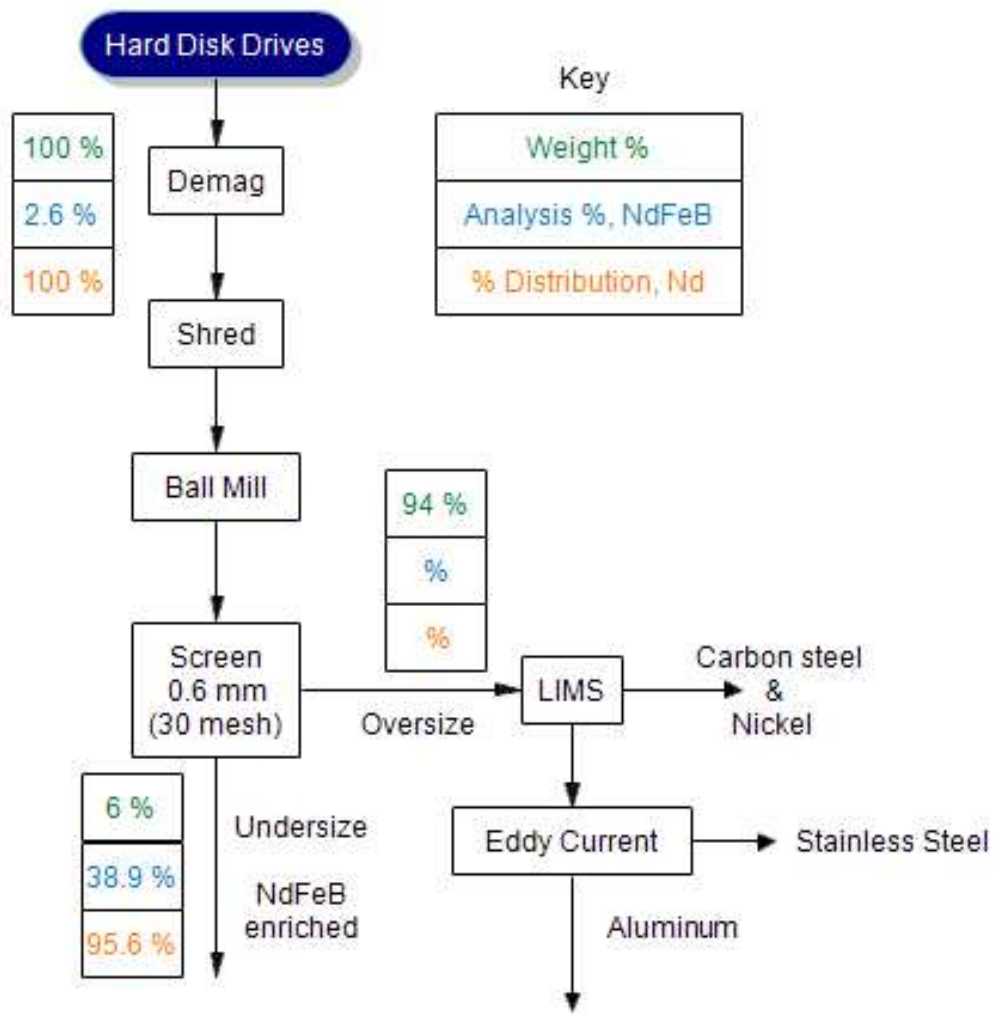


Figure 4.8: Preferential degradation flowsheet.

The upper part of this flowsheet was tested several times to demonstrate the process viability and confirm grade and recovery results observed. The ball mill output The flowsheet presented above demonstrated recovery 96% of the magnet material in the feed at a product grade of 39 Wt.% magnet material.

#### 4.5: Preconcentration by Taking Advantage of Magnetic Behavior

Visual inspection of the shredder product identified clumps of material clustered around magnetic sources. These clusters have been designated as “hairballs.” It was postulated that by separating out these hairballs that magnet material could be concentrated prior to additional processing. This concept was explored including tests to evaluate whether hairballs could be

encouraged to form further by agglomeration in a rolling mill. The agglomeration tests were mostly unsuccessful.

As seen in the disassembly of hard drives the magnet material is associated with the magnet bracket and liberation from that assembly is the largest obstacle to recovery. The magnet bracket is strongly ferromagnetic and therefore reports to the magnetic fraction when processed by a magnetic drum. It was expected that by magnetic pre-concentration (prior to ball milling) barren non-magnetic material could be removed from the process flow prior to costly demagnetization and milling unit operations. It is thought that this can be accomplished while simultaneously producing a higher-grade rare-earth magnet output. The challenge would be accomplishing this without sacrificing recovery.

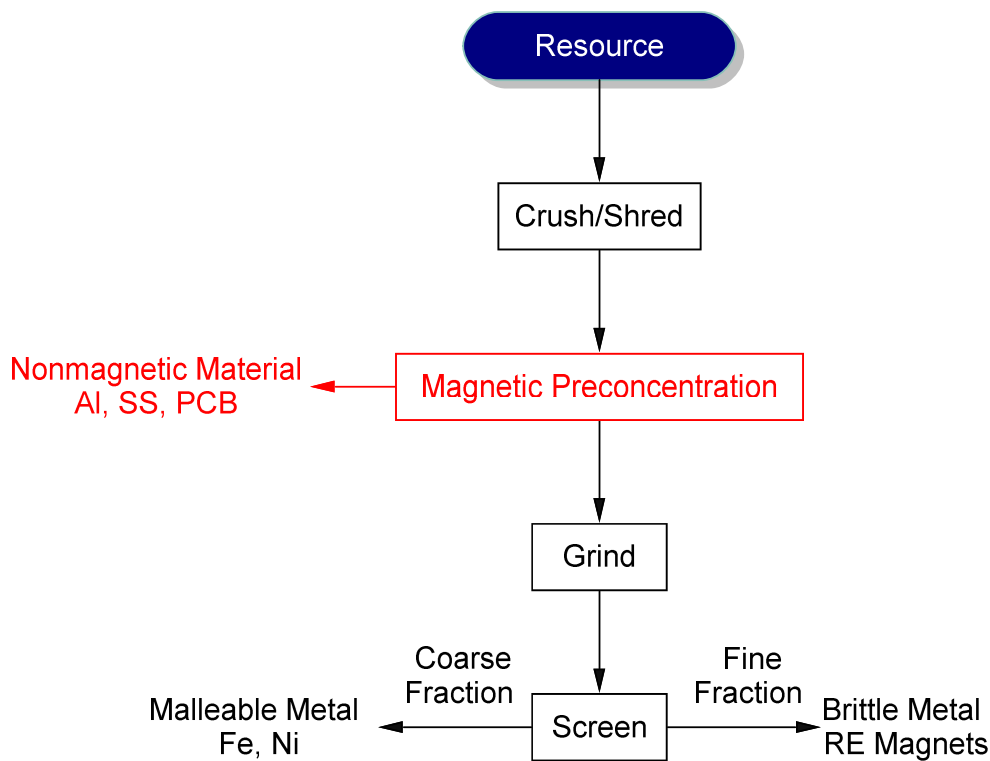


Figure 4.9: Conceptual pre-concentration flowsheet

This was first demonstrated at Laboratory scale (8-inch diameter laboratory grinding mill) with a 3-hard drive sampl. The laboratory mill results showed an increase in product grade while rejecting 70% of the material prior to grinding. This experiment showed a recovery of 92%

of the magnet material with a grade of 75%. This inspired a large, 40 hard sample to be tested. The results of this test can be seen in figure 4.10.

There was a notable loss of recovery between this test and the original preferential degradation flowsheet. Due to this an additional test was completed with a change in process variables. These included increasing the process feed to 80 hard drives. This is due to the lower mass being fed to the ball mill, larger charges were required to maintain the total material mass in the mill as a constant. The low intensity magnet drum was also used rather than the high intensity drum used in the first experiment. This was an attempt to recapture the recovery that was lost by the high intensity magnet. The results of these process variations can be seen in figure 4.10.

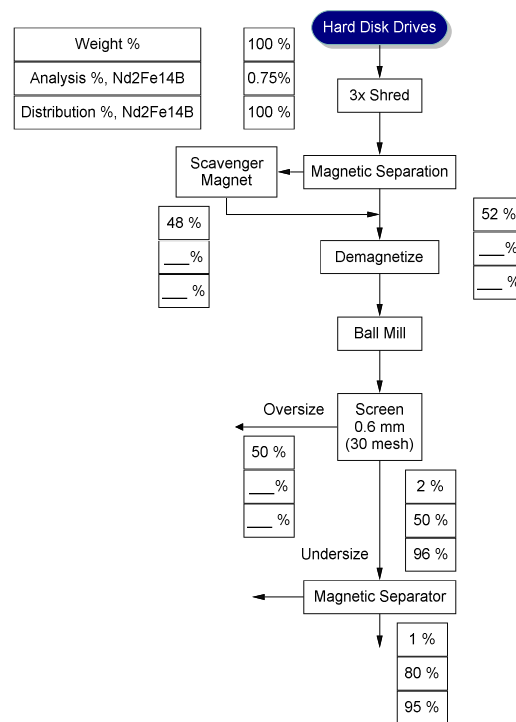


Figure 4.10: Preconcentration flowsheet with results from analysis of outputs

The REE magnet product analyzed at 50 Wt.% Nd2Fe14B leaving the possibility of further upgrading. One possibility is by further low intensity magnetic separation which can be simulated by the Davis tube (wet) separation. The Davis tube shows that magnet material processed by preferential degradation can be concentrated up to a grade of 80 Wt.% just by physical separations.

#### 4.6: Discussion of Co-Products Contributing to Viability of Process

There are two preferential degradation process variations well researched and understood through the research supporting this thesis. The first is a process where shredder output is fed directly into the ball mill for grinding, this is illustrated as figure 4.5. The second variation includes a magnetic preconcentration unit operation prior to the grinding operations. This second variation and its results are illustrated in figure 4.10.

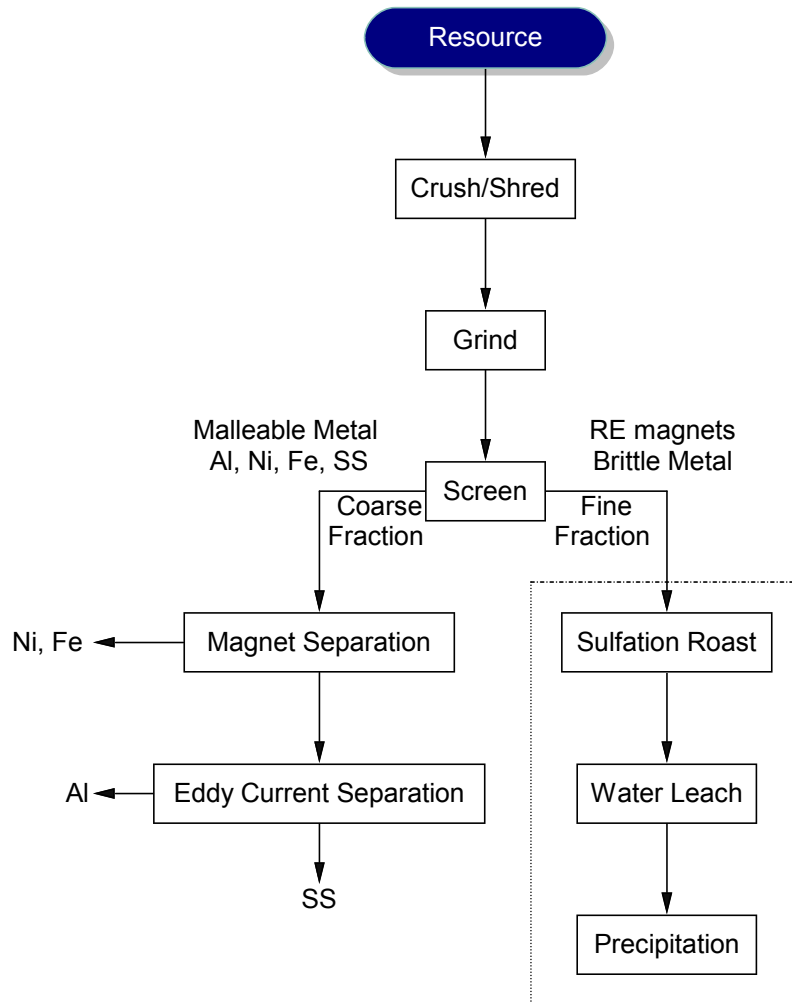


Figure 4.11: Conceptual material destination flowsheet. The further processing of the fine fraction is by a range of processes, for example sulfation roasting.

Both process approaches produce a fine rare-earth magnet enriched product and various nonmagnetic products comprised primarily of malleable metals (Aluminum, Nickel, Steel, Stainless Steel as alloys). The discussion of co-product recovery is presented for these two

flowsheet variations. The economics discussion is based on the pre-concentration flowsheet (figure 4.10).

The coarse fraction is processed differently for the two process variations. The recovery of aluminum, nickel, steel, stainless steel and printed circuit boards is targeted in addition to neodymium recovery.

Recovery of Coproducts from Linear flowsheet:

The process shown in figure 4.5 recovers aluminum, nickel, stainless steel and carbon steel from the ball mill product coarse fraction and recovers neodymium, gold and silver from the fine fraction. The gold and silver are liberated from the printed circuit board. The quantity of contained gold and silver in the fine fraction is determined by fire assay. The results of this assay reveal that gold is present at 230ppm with silver present at 880ppm. The gold and silver may be recovered by any of several processes that are well researched and established. The challenge to gold and silver recovery as is commonly challenging in recycling is achieving the throughput necessary to warrant additional unit operations.

The process postulated for the coarse fraction is separation by high intensity magnet to produce a nickel, steel, stainless steel mixed fraction separate from the aluminum. The aluminum recovery is important as aluminum is among the highest contributors to hard drive recycle value. Industry contact has revealed that the purity of this aluminum is ultimately a non-issue with even significant impurity composition being acceptable. The nickel can be separated from the mixed magnetic fraction using sortation before finally the stainless steel-carbon steel separation is accomplished with low intensity magnet separation.

Recovery of Coproducts from Preconcentration Flowsheet:

The preconcentration flowsheet (figure 4.10) rejects aluminum, printed circuit boards, and plastics before the demagnetization and ball mill unit operations. This nonmagnetic fraction is treated by eddy current separation to produce an aluminum enriched product and a printed circuit board/plastic product concentrate. Both of these fractions are valuable and contribute to the process economics. There are some cases where aluminum and circuit boards are not fully liberated from each other as they have not been ground to the extent as in the process discussed above. The purity of the aluminum fraction is a non-issue as discussed above but recovery of the printed circuit board fraction may impact process economics.

The ball mill output coarse fraction includes steel, stainless steel, and nickel. The steel and nickel can be separated from the stainless steel by low intensity magnet as accomplished above, then the nickel can be separated by sortation. Industrially this sortation is automated but sortation is possible by hand in the laboratory.

These fractions are sorted to estimate the grade and recovery of these materials. The demonstrated recoveries of these materials are shown in table 5.4 below.

Table 4.4: Demonstrated material recoveries of co-products

Material of Interest	Fraction in HDD feed	Demonstrated Recovery
Al	55%	80%
Fe	6%	95%
SS	22%	95%
Ni alloy	8%	90%
PCB	4%	60%
NdFeB	3%	95%

## CHAPTER 5: ECONOMIC CONSIDERATIONS

This research targets the economic recycling of computer hard drives to recover neodymium iron boride magnet material, in addition to other value components, to provide a domestic source for rare earths. The process economics are considered with regard to the viability of the developed processes.

The magnet material output from this process can follow any of several value realization routes, these include but are not limited to; direct reuse of magnet materials, selective sulfation roasting to separate rare earths from iron, or other separations technologies to produce a rare earth oxide concentrate from refined liberated RE magnet powder. The direct reuse of  $\text{Nd}_2\text{Fe}_{14}\text{B}$  material is possible if process output is of a sufficiently high purity grade. This reuse requires less downstream processing and so would be a more valuable process output if grade is shown to be sufficiently high. The minimum output grade for this type of processing is 10 Wt.% neodymium or 27% magnet material.

It is also possible that further refining processes are used on the preferential degradation output such as selective sulfation roasting. There are several of these technologies developed by CMI that have been tested on this process output. Higher grade process output is valuable to

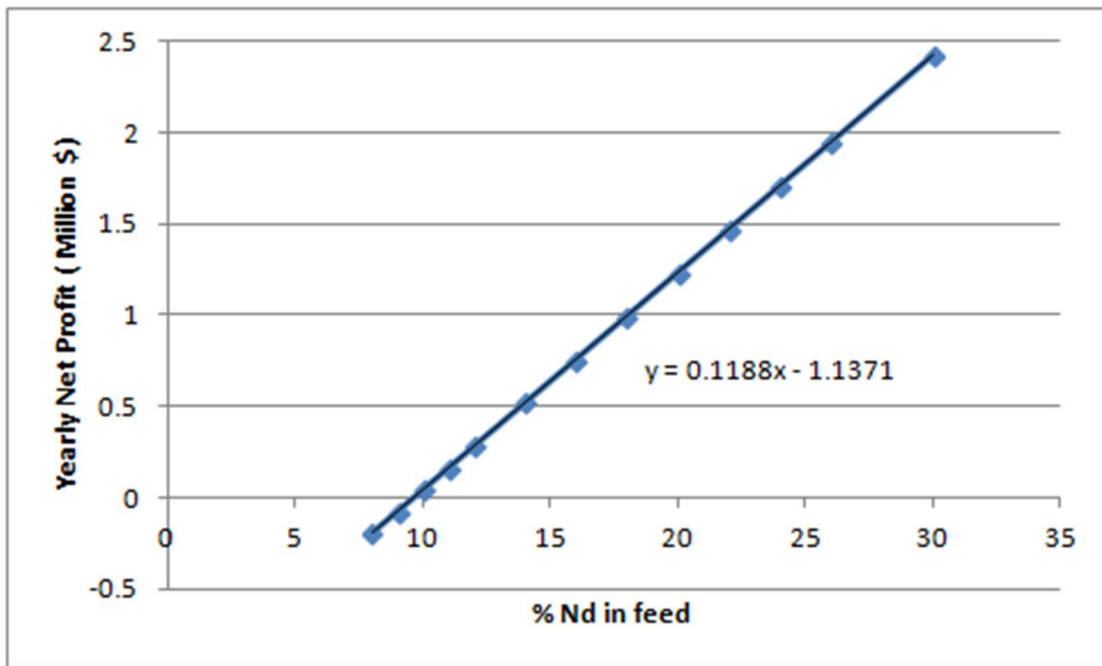


Figure 5.1: Value of neodymium grade for selective sulfation roasting. The minimum cutoff grade for profitability is about 10% neodymium by mass.

these downstream operations as a higher purity feed reduces subsequent reagent consumption and ultimately process costs. The input neodymium grade for selective sulfation roasting is mostly affectual of acid consumption. The economic cutoff for selective sulfation roasting is estimated to be a minimum feed grade of 33% magnet material This is the targeted minimum output grade for the shredder process. The value of increasing the preferential degradation product grade (for selective sulfation roasting) is shown in the figure XX.

**5.2: Hard Drive Valuation**

Material value estimates are based on documented recycle price when available. This is true for the carbon steel, stainless steel, aluminum, and nickel alloy value fractions output from the processes outlined above. The neodymium iron boride value is based on an industrial partner’s recent purchase of a magnet material block.

Table 5.1: The values of the materials found in hard disk drives. These are reduced in for estimation of revenue to represent uncertainty and impurities.

Material of Interest	Value(\$/lb)
Al	\$0.40
Fe	\$0.15
SS	\$0.61
Ni alloy	\$4.25
PCB	\$3.50
NdFeB	\$5.00

The value for printed circuit boards (PCB) is initially based on recycle value of printed circuit boards quoted from recyclers around the United States including in Tennessee, California, and Colorado. The printed circuit boards are also analyzed for precious metals composition by

Table 5.2: Printed circuit board value based on fire assay results. This represents the total entrained commodity value and must be reduced to represent the challenges of recovery from the circuit board. The value displayed in table 5.1 is based on this data.

	PPM	g/hdd deskstar	value per gram	encased value per HDD	Total value per lb:
Ag	1560	0.053	\$0.52	\$0.03	\$0.37
Au	453	0.015	\$42.18	\$0.65	\$8.67
Total				\$0.68	\$9.04

fire assay. The range of values quotes from recyclers is from \$0.10 to \$15.00 per lb. This varies mostly based on geographic location and on circuit board type. Some jurisdictions have legislation in place that mandates recycling of circuit boards and in these regions, it is not uncommon for recyclers to charge for circuit board disposal or at least to not pay for their

Table 5.3: The entrained circuit board value from previous research. [16]

<b>Metal</b>	<b>Market price per unit (USD)</b>	<b>Unit</b>	<b>Average composition (%)</b>	<b>Market value per tonne of PCBs (USD)</b>
<b>Gold</b>	41.5	g	0.0191	7,927
<b>Silver</b>	0.54	g	0.0618	334
<b>Palladium</b>	32.5	g	0.0124	4,030
<b>Copper</b>	7	kg	21.5	1,505
<b>Tin</b>	20	kg	4.09	818
<b>Lead</b>	2	kg	2.77	55
<b>Zinc</b>	3	kg	1.34	40
<b>Nickel</b>	11	kg	0.85	94
<b>(Source: InvestmentMine Daily Metal Spot Price, December 1<sup>st</sup> 2017)</b>				
<b>Total market value per tonne of PCBs (USD)</b>				14,802

acquisition. Some printed circuit boards are known to have much higher gold and precious metals content. The literature also included analysis of the composition of printed circuit boards containing gold, silver, and platinum entrained value. The range of literature supported values for printed circuit boards is from \$0.15 to \$10.00.

Printed circuit boards from 3 hard drives were removed from the hard drives by disassembly and ground using a laboratory rod mill. The ground material was assayed by fire assay to determine the amount of gold and silver in the circuit board samples. This study showed that the PCBs from the disk drives, those that would be expected to be processed, have a composition containing about 450ppm gold and 1560ppm silver. A fraction of 40% of this value is used as the value of PCBs to represent the recovery and processing costs to extract those precious metals from circuit boards. This estimate shows that the PCB value is approximately \$3.50 per pound.

The value per hard drive is highly dependent on the recycle material value of aluminum, nickel alloy, stainless steel, printed circuit boards, and magnet material as well as the recovery of

those materials. The metals recovery is analyzed by hand sorting the identifiable materials in a specific fraction and massing the relative amounts of each material present in each fraction.

Table 5.4: Table of Recovered Value from shredded hard drive process on a per

Material	Fraction of HDD	Encased Value	Recoverd Value
Al	55%	\$0.22	\$0.18
Fe	6%	\$0.01	\$0.01
SS	22%	\$0.18	\$0.17
Ni	8%	\$0.40	\$0.36
PCB	4%	\$0.18	\$0.11
NdFeB	3%	\$0.15	\$0.14
Total:		\$1.13	\$0.96

The demonstrated recoveries of materials in conjunction with their quoted values allows an estimate of the value of materials composing hard drives. Individual hard drive models are disassembled into component pieces to analyze their potential value. This analysis included 26 hard drive specimens with 19 specimens representing a sample from a 4300 HDD lot. This analysis allows a representative average to be constructed from the count of hard drives matching each model in the lot. The average hard drive value is calculated to be \$0.96 per hard drive and \$1450 per ton. These numbers are based on the demonstrated recoveries of materials found in the hard drive construction, therefore this could be considered the recoverable value of processed hard drives.

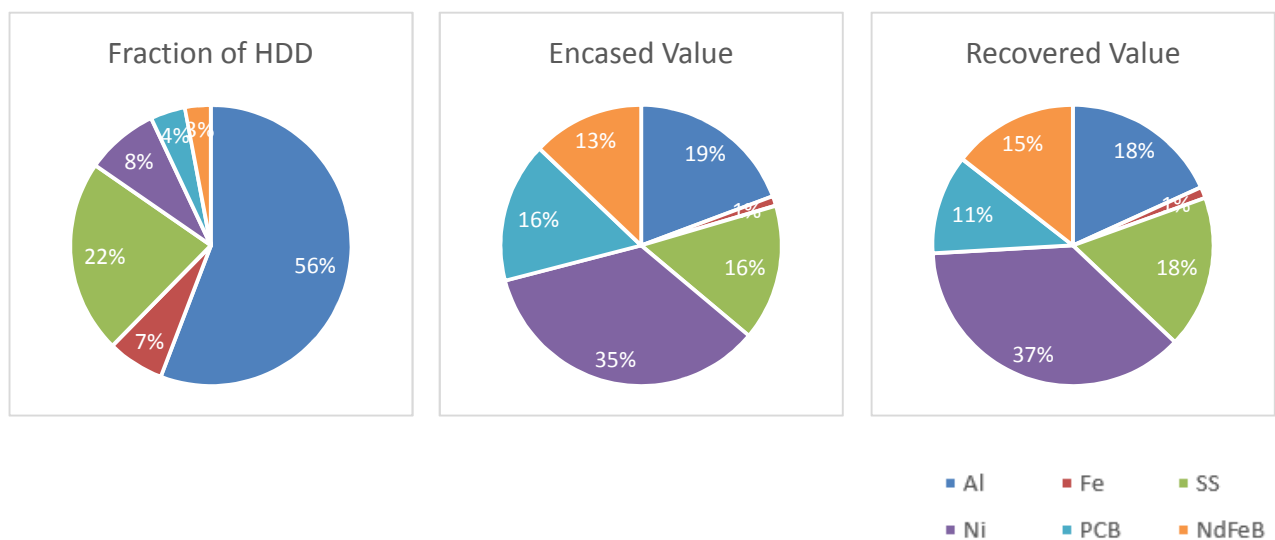


Figure 5.2: Charts showing the material composition, inherent value, and recovered value

The total material value of the average hard drive is \$1.13 which equates to \$1700 per ton. Based on the demonstrated recovery it can be estimated that 85% of the total hard drive value is recovered. The demonstrated recoveries are used for revenue estimates in the cost model below. The hard drive value is sensitive to recycle values of stainless steel, aluminum, nickel alloy, printed circuit board and magnet material ( $\text{Nd}_2\text{Fe}_{14}\text{B}$ ).

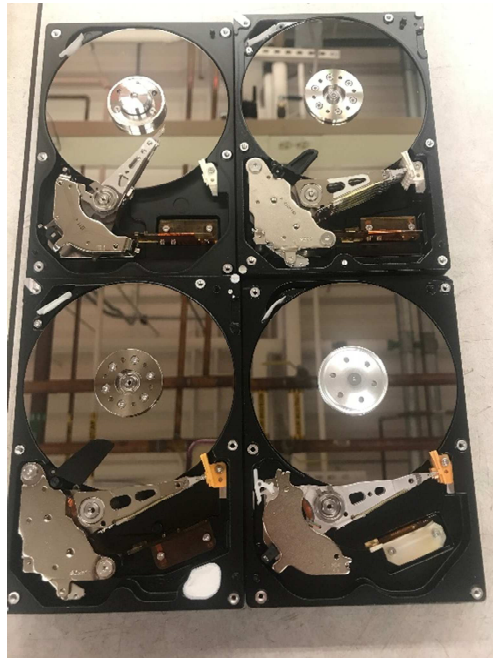


Figure 5.3: Hard drives from a range of years. Clockwise from top left: 2003, 2008, 2011, and 2010. All Hitachi deskstar model hard drives.

The magnet composition from several of these disassembled drives is analyzed. It is found that composition varies considerably with brand. These ranges of magnet mass in the total hard drive are represented in the average discussed above however the value of the neodymium in the process output might vary significantly. It seems that dysprosium or praseodymium must be increased in response to a decrease in the neodymium composition. This data suggests that for mixed hard drive process feed that monitoring the neodymium in the process output may not fully account for the magnet material.

Table 5.5: composition data of magnets from several manufacturers.

Brand	Model	Magnet Mass	Fe composition	Nd composition	Pr composition	Dy composition
Seagate	Barracuda	20.2724	62.6156	21.8414	5.8042	1.3084
Western Digital	Caviar Blue	4.7572	65.1091	27.7560	0.128	2.0858
Western Digital	Caviar Green	5.082	65.2929	26.5636	0.0611	2.9025
Hitachi	Deskstar	22.02704	65.7426	27.6098	0.0834	1.3432

Hard drive specimens of the same make and model from select years are disassembled and analyzed as described above. This analysis included Hitachi Deskstar hard drives from 2003, 2008, 2010, and 2011. The evaluation of these hard drives contributes some evidence to the change in value of hard drives over several years. The data from this analysis can be seen in table 5.6 below.

Table 5.6: Deconstruction results of the 4 hard drives shown above. The matrix on the left shows the mass breakdown of each drive. The matrix on the right shows the value of those components and the total value of the drive.

	2003	2008	2010	2011		2003	2008	2010	2011
Al Fraction	51%	56%	61%	67%	Al fraction	\$0.15	\$0.22	\$0.22	\$0.14
Fe Fraction	0%	0%	0%	0%	Fe Fraction	\$0.00	\$0.00	\$0.00	\$0.00
SS Fraction	37%	27%	23%	23%	SS Fraction	\$0.26	\$0.26	\$0.20	\$0.12
Ni alloy Fraction	6%	8%	8%	4%	Ni alloy Fraction	\$0.26	\$0.43	\$0.40	\$0.12
PCB Fraction	4%	5%	3%	4%	PCB Fraction	\$0.16	\$0.18	\$0.04	\$0.03
NdFeB Fraction	1%	3%	3%	1%	NdFeB Fraction	\$0.05	\$0.17	\$0.17	\$0.02
Total Mass	549.5	750	673	394	Total Value	\$0.88	\$1.26	\$1.03	\$0.43

Table 5.7: Circuit board values from Hitachi Desk-Star hard drives with various dates of manufacture.

Year	Gold PPM	Silver PPM	Encased Value
2003	712	1336	\$13.93
2008	453	1560	\$9.04
2010	177	893	\$3.60

The variation in constituent material content over time can be observed in the context of the market conditions including the 2010-2011 rare earth crisis. The drastic reduction in neodymium consumed in a hard drive between 2010 and 2011 is attributed to this event. There is insufficient evidence to suggest whether this pattern continues. There are conclusions that can be drawn into the future. The analysis of the separate fractions in the hard drive are completed considering them as fractions of the whole hard drive. It is expected that throughput would be a consistent mass on a yearly basis rather than based on the number of drives processed. The total mass of a drive is less important than the material value per ton in the feed source. The value per ton does decrease over the range of dates selected. That value for the 4 years are \$1450, \$1500, \$1390, \$992 per ton. The 2008 hitachi desk-star is above average in terms of value. It appears that the aluminum composition of the drive increases over time and that the amount of stainless

steel is reduced over time. This trend is likely due to the general trend toward increasing the number of platters per drive to increase storage capacity. If this pattern holds true across several hard drive brands into the future it may suggest that the preconcentration to remove the nonferrous material from the ball mill feed would be further advantaged in the future. The printed circuit board mass as a fraction of the total drive mass remains similar throughout the range for which there is data. However, the value of the printed circuit boards is analyzed by fire assay as conducted above. The boards from the 2003 and 2010 drives are pyrolyzed, ground, and fire assayed. The 2011 circuit boards are expected to be similar in composition to the 2010 drive, therefore the value determined from the 2010 circuit board is used. This data is used to calculate the values in table 5.6. If this pattern continues the benefit to improved circuit board recovery may be limited. Table 5.7 shows the encased value of gold and silver in circuit boards based on the manufacture date of their respective hard drives.

Literature survey and industry contacts identify a per hard drive shredding value as a service charge. This value is significantly greater than the recovered material value. The literature supports a service charge of up to \$12 per hard drive. The nominal service charge is identified at \$5 per hard drive and this value is used for comparison to other CMI projects. The Economic analysis considers a case of \$0 for the shredding service charge to illustrate a minimal value of recycling. The \$5 service charge case is also evaluated as part of the sensitivity analysis to illustrate the change in revenue and sensitivity to shredding charge.

### 5.3: Estimation of Major Costs

Capital expenditure or CAPEX is estimated using quotes on process equipment from manufacturers on major line items and using Costmine for minor capital items. The capital breakdown for the plant is shown in table 5.8. [19] The major line items for capital equipment are the shredder, ball mill, furnace, and materials handling equipment costs. There are additional line items built into the estimate for space and facilities. The equipment delivery and installation, plant engineering and construction, electrical and plumbing installation, and equipment instrumentation are estimated using capital cost estimation from factors provided in Mineral Processing Plant Design, Practice, and Control. Or factors used commercially by TetraTech inc per Erik Spiller. [17] When provided a range for these values, the highest value was selected, this was due to the small plant size as such the various costs could be expected to be a higher fraction of the total plant value. The plant designed is disadvantaged due to the relatively small scaled

Table 5.8: Capital expenditure (CAPEX) table. Major equipment costs are based on manufacturer budgetary prices. Cost factor calculations are used to determine various additional capital costs.

Cost Item	Budget Price
Feeder	\$ 10,200
Shredder	\$ 300,200
Demag Furnace	\$ 75,000
RE drum sep	\$ 27,000
Eddy Current Sep	\$ 46,000
Batch BM	\$ 89,700
grizzley	\$ 35,000
Screen	\$ 55,500
Fume Control Scrubber	\$ 27,500
Bag House	\$ 27,300
Materials Handling	\$ 103,200
Space	\$ 108,700
Subtotal:	\$ 905,300
Delivery	\$ 27,159
Construction:	
Engineering	\$ 298,749
Contingency:	
Property	\$ 500,000
Sum (initial estimate)	
Installation	\$ 226,325
Electrical	\$ 226,325
Instrumentation	\$ 90,530
Subtotal 2	\$ 2,274,388
Operating Capital	\$ 207,109
Total With Contingency	\$ 3,280,000

compared to mining operations. The estimates provided include a 35% contingency for the CAPEX value. The CAPEX value is estimated between \$2.6Million and \$3.3Million depending on which specific set of factors is used. The higher estimate using the textbook (Mineral Processing Plant Design, Practice, and Control) factors is used for the following calculations and conclusions for demonstration of the process economics. There is a range of uncertainty expected with this estimate due to uncertainty in process variables as well as uncertainty specific costs. The operating expenditure or OPEX value is estimated mostly from Costmine. The OPEX is broken down into 3 main categories; Labor, power, and consumables. Labor is estimated from Costmine data for national average hourly wage rates for mill laborers. The labor cost includes 2 mill laborers and a shift foreman as well as the cost for a business manager and a sales representative. The Energy costs are based on using average nationwide electrical energy sales values; for this estimate the energy costs are based on quoted horsepower values for the various equipment. The demagnetization furnace in this cost model is an electric box furnace. When this base case is compared to a model using a natural gas furnace, there is an increase in capital

Table 5.9: Operating expenditures. The HDD delivery, labor, and electric power contribute most significantly to the cost.

Cost Item:		per unit cost	total cost/unit	units per year	Total per year:
<b>LABOR:</b>	Quantity	cost per hour		units per year	<b>\$536,094.00</b>
laborers	2	\$22.62	65.598	2000	\$131,196.00
foreman	1	\$24.62	\$35.70	2000	\$71,398.00
business manager	1	\$65.00	94.25	2000	\$188,500.00
Sales/Purchasing Rep	1	\$50.00	72.5	2000	\$145,000.00
<b>ELECTRIC POWER</b>	<b>QNTY per Hr (Kw)</b>	<b>cost per KwHr</b>		<b>units per year</b>	<b>\$78,576.01</b>
Ball Mill	14.92537313	\$0.07	1.07761194	1000	\$1,077.61
Shredder	224	\$0.07	16.1728	2000	\$32,345.60
Screen		\$0.07	0	2000	\$0.00
Furnace	100	\$0.07	7.22	4000	\$28,880.00
Converyor	15	\$0.07	1.083	2000	\$2,166.00
Scrubber	7	\$0.07	0.5054	2000	\$1,010.80
Contingency Factor					\$13,096.00
<b>SCREEN:</b>		cost per ton		units per year	<b>\$ 2,880.00</b>
screen inserts	32	\$45.00		2	\$2,880.00
<b>BM consumables:</b>		cost per ton			<b>\$ 1,884.80</b>
Balls	1520	\$1.15			\$1,748.00
Liners	1520	\$0.09			\$136.80
<b>HDD Delivery:</b>	<b>1900000</b>	<b>\$0.11</b>			<b>\$209,000.00</b>
<b>Total:</b>					<b>\$ (828,000.00)</b>

expenditure relative to the base case but the operating expenditure is reduced as the energy cost is less for natural gas than for electric power. It is expected that a gas furnace would evolve more off gas and require a higher volume scrubber as well. The model is not well enough developed at this stage to warrant decision making between different furnace types, therefore, for the purposes of the analysis and conclusions herein, the base case with an electric furnace is used. The interval analysis of this process variation can be completed when the operating and capital expenditure is further refined in the estimate. The Operating expenditure used for the cost model below is estimated at \$830K per year. [18]

The plant life for economic purposes is estimated at 10 years. This longevity impacts the value as well as the per hard drive cost. A longer plant life would reduce the processing cost per hard drive as the capex would be distributed across a greater number of hard drives. The plant life also impacts the net present value of the project. The plant is designed for an annual throughput of 1.9 million hard drives.

Table 5.10: Model including both operating and capital expenditures in the appropriate time periods from the estimates discussed above.

	Year 0	Year 1	Year 10
Capex:	\$ (3,280,000.00)		
Opex:		\$ (828,000.00)	\$ (828,000.00)

The cost per hard drive is determined by dividing the net present cost (NPC) over the throughput for the estimated plant life. The NPC is determined below. It is necessary to turn the future costs into a present value by using price value factors. [19]

$$Net\ present\ cost = Capex + Opex * \left( \frac{P}{A_{.10,10}} \right) * \left( \frac{P}{A_{.10,1}} \right) \quad (5.1)$$

The factor  $F/A_{i,n}$  turns an annual cashflow into a single cashflow at the beginning of the constant cashflow period. The second factor  $P/A_{i,n}$  brings that single cashflow into the time period 0. The factor  $I$  represents the rate of return expected, while the factor  $n$  represents the time period over which the factor is applied. The factors can be calculated but are usually based on tables, for this research the tables in Economic Evaluation and Investment Decision Making (14<sup>th</sup> edition) was used to determine these factors. The net present cost is \$8.2million. This represents the total cost for processing 10 years of throughput including the CAPEX and OPEX costs. This is in terms of present dollars.

By dividing the net present cost by the designed throughput of 1.9million HDDs annually over a 10-year plant life the per unit HDD processing cost is found to be \$0.43. This is useful for comparison to other projects with different combinations of year 0 capital expenditure and per unit operating costs.

**5.4: Revenue and Process Net Present Value**

The recycled value using demonstrated recoveries and materials value as discussed above is \$0.96 per hard drive. That value compared to the processing cost shows that hard drives can be recycled economically. The value of average hard drives as discussed above is used to calculate the revenue based on recycling average computer hard drives. This revenue is \$0.96 per hard drive which leads to a net revenue estimate of \$1.8million annually. The cash flows are evaluated before tax to demonstrate the value of the project.

Figure 5.11: Cashflow model

	Year 0	Year 1	Year 10
Capex:	\$ (3,280,000.00)		
Opex:		\$ (828,000.00)	\$ (828,000.00)
Revenue:		\$ 1,825,000.00	\$ 1,825,000.00
BTCF:	\$ (3,280,000.00)	\$ 997,000.00	\$ 997,000.00

The cash flow model shows the estimated future cashflows including revenue from hard drive processing and operating expenditure. The future cashflows are based on revenue minus operating expenditure. The operating expenditure calculation and considerations are discussed above in section 5.3. The revenue is based on the per hard drive recovered value multiplied by the designed annual throughput of 1.9million hard drives. For the purposes of the initial revenue estimate a shredding charge is not considered and only recycle revenue is included. The shredding charge does not affect the conclusion in this initial estimate and sensitivity to the shredding charge is discussed below. The shredding charge is not well understood as A) market surveys of disperse user shredding service charges are not considered representative of larger scale users and B) the charge is extremely variable among different locations. The values are converted to present values using payment interest factors. The Net present value and IRR is evaluated to determine the project viability. The net present value is evaluated using multiple discount rates of 5%, 10%, and 15%. This is done to show that the project is profitable over a range of internal rates of return. The rate of return is also determined to demonstrate the interest

rate at which the project present value is zero. The net present values for these three discount rates are; \$4.8million, \$2.9million, and \$1.7million, respectively. The rate of return analysis indicates that a rate of return of 28% is expected for the plant as designed above (section 5.4). This analysis allows a conclusion to be drawn on the profitability of a plant following the processes developed herein. As stated above this conclusion is drawn without the inclusion of a shredding charge. It can be stated that solely based on the recovered value the process is profitable. The shredding charge is expected to be positive so the addition of such a charge would benefit the projected net present value. This is a before tax calculation and business decisions should include the assessment of expected taxes as part of the refinement of this cashflow model.

### **5.5: Sensitivity Analysis**

The sensitivity of the process economics to several variables is considered below. The factors considered include various costs, project life, recovery and value of products, and service charge. These analyses do not include any probabilistic considerations and are exclusively to illustrate the change in process values based on changes in certain parameters. The graphs could contribute to discussion of the economic and technological challenges remaining for implementation. The base case for all conditions is that shown in the cashflow model above. The effect of changes in each parameter are computed while maintaining all other variables constant. The graphs are drawn such that the percent change in net present value is plotted as the dependent variable while the percent change in the driving variable is plotted on the horizontal axis. For all of these graphs the net present value is based on a discount rate of 10%. This analysis could be completed using other values for the discount rate and would change the analysis to some degree. A higher discount rate would favor present period values and result in greater discount of future values. The graphs in this section are generally produced such that the discount rate would affect the sensitivity evenly on individual graphs. The exception to this is the cost sensitivity diagram in Figure 5.4. This figure shows the sensitivity to changes in labor cost, energy costs and capital expenditure.

The process economics are relatively insensitive to energy costs compared to labor, capital, and delivery expenditures. These three operating costs (labor, delivery, and energy) are responsible for the vast majority (99%) of the operating cost estimate, so other operating costs are not considered for the purposes of this sensitivity analysis. The Capital expenditure is not subject to

change based on discount rate as the cashflow model above considered capital in the current period. The operating expenditures are discount rate dependent as they affect future time period cashflows. Energy savings capital expenditures were discussed including the use of a natural gas furnace rather than an electric oven for demagnetization, the benefit of this should be explored with a more refined economic model. Changes in labor can be expected based mostly on plant location. Certain jurisdictions have higher average incomes and would therefore contribute to a higher cost for laborers. For the base case average wages for mill laborers across the United States were used, this could be higher or lower depending on plant location. The Delivery charge is subject to change based on petroleum price, the total is also subject to change based on process throughput. Capital costs can change significantly from this initial economic examination. It should be noted that the sensitivity reflects both consumption and per unit cost. For instance, an additional employee would contribute to variation in the labor cost in the same way as a higher wage rate for those included. This diagram enables discussion of either of those changes as a percentage of the base case total labor cost.

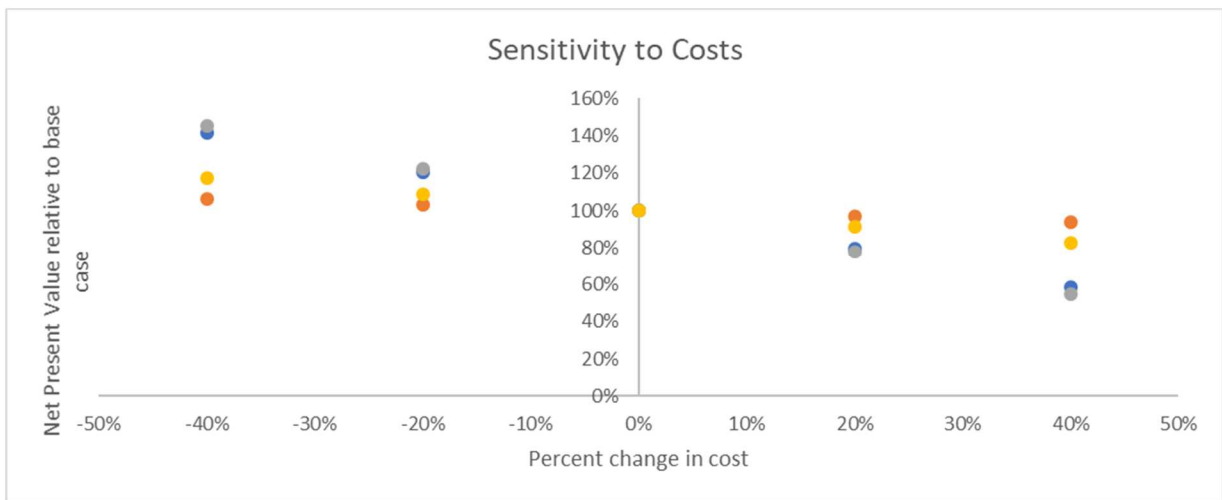


Figure 5.4: Sensitivity of net present value to various costs

Material recovery from the hard drive feed is expected to affect the process value. The base case is calculated using the demonstrated recoveries above (figure 4.4) with the average hard drive composition used as the feed composition. The sensitivity represents a relative change of the recovery value of each material. The chart effectively illustrates the value of improved recovery of each component. Conversely the graph also illustrates the cost of lost recovery. It is

shown that the net present value is most sensitive to the recovery of Aluminum, stainless steel, magnet material, and printed circuit board in order. This indicates which materials recoveries are most beneficial to be improved. The recovery of steel is relatively ineffectual to the project economics.

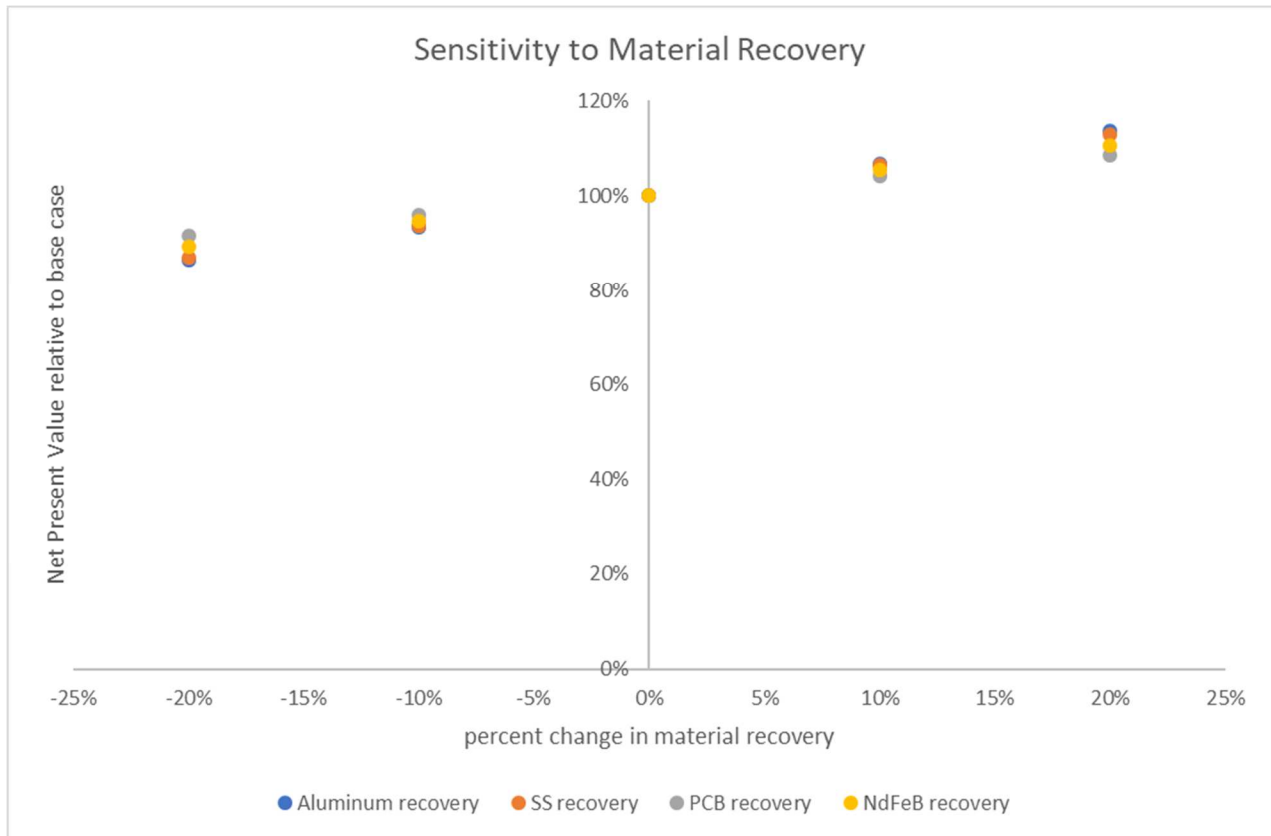


Figure 5.5: Sensitivity of net present value to material recoveries

The effect of changes in material value would respond similarly to what is shown in figure 5.5. The material value sensitivities are very similar to recovery sensitivities. Changes in material value should be expected especially for the rare earth containing magnet material. The larger volume commodities, aluminum, steel, and stainless steel are less likely to vary due to changing market conditions, however these material values can vary somewhat depending on location.

The cashflow model is also sensitive to project life, Figure 5.6 shows the sensitivity of process net present value to project life. The range of project lives from 6 to 14 years is shown in

this graph. The project life would also affect the per hard drive processing cost as shorter project lifetimes would amortize the initial capital expenditure over a fewer number of hard drives. Throughput is expected to affect the process economics positively. The analysis of throughput is dependent on the scaling of CAPEX and OPEX values. With additional research this could be considered. Without understanding of how these costs scale the sensitivity analysis is

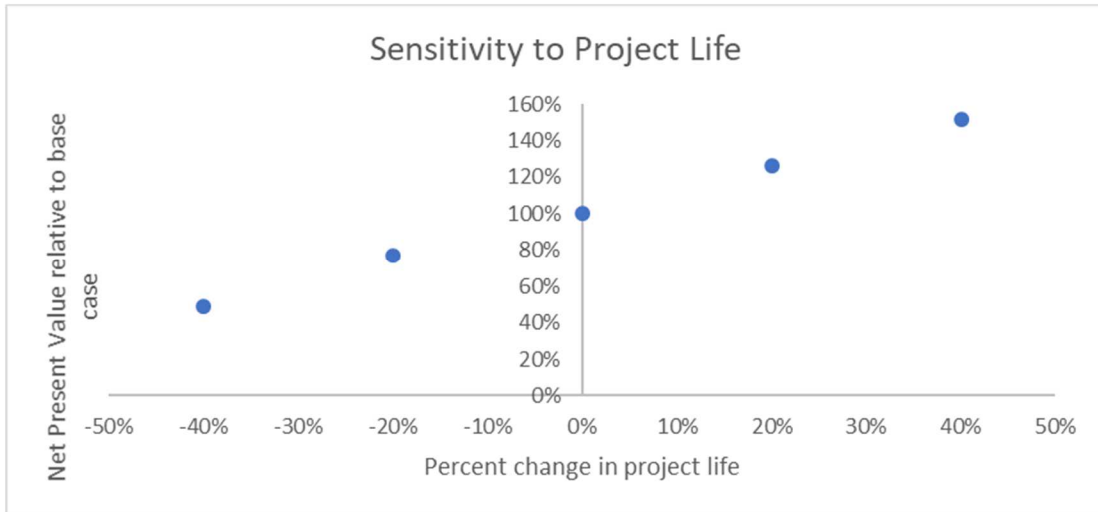


Figure 5.6: Sensitivity of net present value to project life

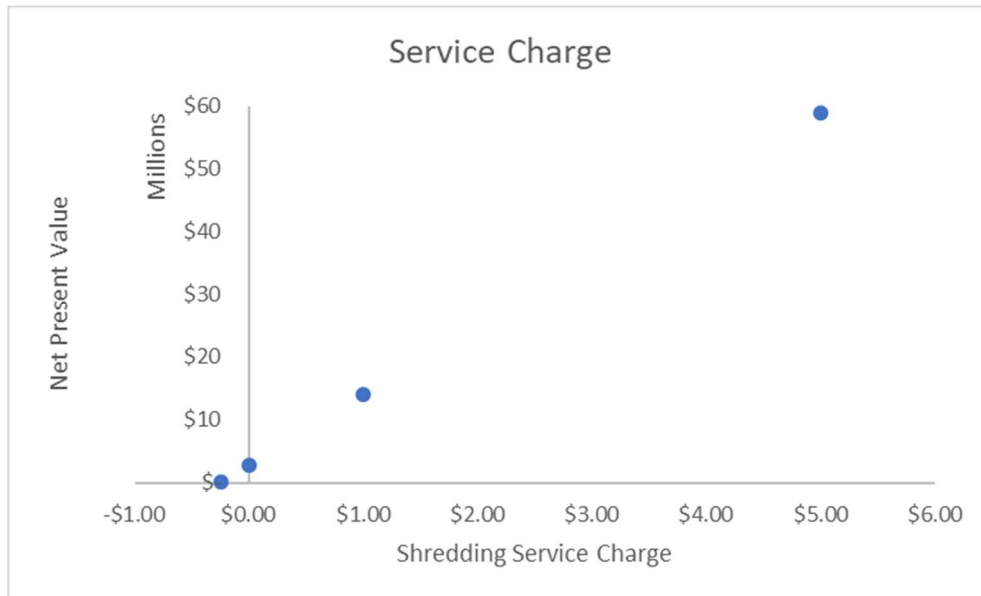


Figure 5.7: Sensitivity of NPV to service charge.

The final parameter evaluated for sensitivity is the service charge. The base case used for conclusions in section 5.4 above is based on a model with a \$0 service charge. This analysis shows that the process is profitable even without a shredding charge. A range of shredding charges are evaluated, these include the case of a typical service charge of \$5 used for comparison to other CMI projects. The highest charge supported by literature search is \$12 per drive. This is not a common case but represents the upper limit of the shredding charge. This analysis is extended to the case where hard drives must be purchased for the recycle process. The breakeven cost for purchased hard drives is about \$0.26 per drive.

## CHAPTER 6: CONCLUSIONS AND DIRECTION FOR FUTURE RESEARCH

The development of a process for the recovery of neodymium, considered a critical material, from recycling of computer hard drives is discussed and evaluated. The process developed takes advantage of the brittle nature of the neodymium magnet material when presented to a grinding mill to produce a fine product composed primarily of powdered magnet material. The economics of hard drive recycling are considered in a preliminary technical economic analysis of the process designed. Based on demonstrated results from tests on 35kg samples the demonstrated recoveries coupled with value estimates can be used to estimate the profitability of this process. The recovery of rare earth bearing magnet material is demonstrated with mixed hard drive feeds. The economic model shows preliminary economic viability and indicates technical and business parameters that should be the direction of future research. The produced  $\text{Nd}_2\text{Fe}_{14}\text{B}$  material grade is sufficient for economic reduction to produce pure or mixed rare earth oxides. The total recovery of magnet material is 96% at a grade of 50 Wt.% magnet material. Maximum output grade is demonstrated at 80% magnet material by weight.

### **6.2: Direction for future research:**

Further research includes both technical refinement of the process as well as variations of business decisions. The technical research should focus on determining more precise process design criteria including such criteria as ball mill residence time, demagnetization time and temperature, degradation of ball mill liners and balls, and wear rate of the various screens. Several business parameters should be more precisely decided as well. Particularly a known plant location would enable a more accurate economic analysis via refinement of the estimate of labor costs, energy costs, and shipping costs. Shipping costs particularly are impactful of the per hard drive profit margin. As seen in the sensitivity analysis shredding charges are very impactful and accurate estimates of the shredding charge would enable a better model to be produced. Expansion to additional magnet bearing devices should be considered. The magnet's brittle nature is expected regardless of the specific device containing the magnet. It is possible that the preferential degradation type process can be applied to a range of devices for REE recovery. There is particular advantage to the process product being suitable for direct reuse as a bonded or sintered magnet. It is expected that the demonstrated recovery is of material that is significantly oxidized. Consideration should be given to grinding, screening, and other process steps under an inert gas cover gas to maintain the magnet material compound.

## REFERENCES

- [1] U.S. Department of Energy - Critical Materials Strategy. Washington, D.C.: United States. Dept. of Energy. Office of Energy Efficiency and Renewable Energy, 2010.
- [2] V. Zepf, *Rare earth elements*. Berlin: Springer, 2013.
- [3] B. Sprecher, R. Kleijn and G. Kramer, "Recycling Potential of Neodymium: The Case of Computer Hard Disk Drives", *Environmental Science & Technology*, vol. 48, no. 16, pp. 9506-9513, 2014.
- [4] X. Du and T. Graedel, "Global Rare Earth In-Use Stocks in NdFeB Permanent Magnets", *Journal of Industrial Ecology*, vol. 15, no. 6, pp. 836-843, 2011.
- [5] J. Rademaker, R. Kleijn and Y. Yang, "Recycling as a Strategy against Rare Earth Element Criticality: A Systemic Evaluation of the Potential Yield of NdFeB Magnet Recycling", *Environmental Science & Technology*, vol. 47, no. 18, pp. 10129-10136, 2013.
- [6] A. King, R. Eggert and K. Gschneidner Jr., *Handbook on the Physics and Chemistry of Rare Earths*, 50th ed. 2016, pp. 19-46.
- [7] T. G. Gutowski and J. B. Dahmus, "Mixing entropy and product recycling," *Proceedings of the 2005 IEEE International Symposium on Electronics and the Environment, 2005.*, 2005, pp. 72-76.  
doi: 10.1109/ISEE.2005.1436997
- [8] C. Shaneyfelt, B. Jeffers and D. Imholte, Critical Materials Institute Annual Meeting, Oak Ridge, TN, unpublished research, 2016.
- [9] M. Ueberschaar and V. Rotter, "Enabling the recycling of rare earth elements through product design and trend analyses of hard disk drives", *Journal of Material Cycles and Waste Management*, vol. 17, no. 2, pp. 266-281, 2015.
- [10] D. München and H. Veit, "Neodymium as the main feature of permanent magnets from hard disk drives (HDDs)", *Waste Management*, vol. 61, pp. 372-376, 2017.
- [11] S. Abrahami, Y. Xiao and Y. Yang, "Rare-earth elements recovery from post-consumer hard-disc drives", *Mineral Processing and Extractive Metallurgy*, vol. 124, no. 2, pp. 106-115, 2014.
- [12] O. Takeda, T. Okabe and Y. Umetsu, "Recovery of neodymium from a mixture of magnet scrap and other scrap", *Journal of Alloys and Compounds*, vol. 408-412, pp. 387-390, 2006.
- [13] K. Baba, Y. Hiroshige and T. Nemoto, "Rare-earth Magnet Recycling", *Hitachi Review*, vol. 62, no. 8, pp. 452-455, 2013.
- [14] H. Bandara, J. Darcy, D. Apelian and M. Emmert, "Value Analysis of Neodymium Content in Shredder Feed: Toward Enabling the Feasibility of Rare Earth Magnet Recycling", *Environmental Science & Technology*, vol. 48, no. 12, pp. 6553-6560, 2014.

- [15] A. Walton, H. Yi, N. Rowson, J. Speight, V. Mann, R. Sheridan, A. Bradshaw, I. Harris and A. Williams, "The use of hydrogen to separate and recycle neodymium–iron–boron-type magnets from electronic waste", *Journal of Cleaner Production*, vol. 104, pp. 236-241, 2015.
- [16] H. Cui and C. Anderson, *Hydrometallurgical Treatment of E-scrap*, P.h.D. Dissertation, Colorado School of Mines, 2018.
- [17] *Mine and mill equipment cost*. Spokane Valley, Washington: InfoMine USA, 2012.
- [18] A. Mular, D. Halbe and D. Barratt, *Mineral processing plant design, practice, and control*. Littleton: Society for Mining, Metallurgy, and Exploration, 2002.
- [19] F. Stermole and J. Stermole, *Economic evaluation & investment decision methods*. Lakewood: Investment Evaluations Corp., 2014.